



**HAL**  
open science

# (SI) Applications of analytic and geometry concepts of the theory of Calculus of Variations to the Intrinsic Reaction Coordinate model

Josep Maria Bofill, Antoni Aguilar-Mogas, Xavier Giménez, Ramon Crehuet

► **To cite this version:**

Josep Maria Bofill, Antoni Aguilar-Mogas, Xavier Giménez, Ramon Crehuet. (SI) Applications of analytic and geometry concepts of the theory of Calculus of Variations to the Intrinsic Reaction Coordinate model. *Molecular Physics*, 2008, 105 (19-22), pp.2475-2492. 10.1080/00268970701519762 . hal-00513124

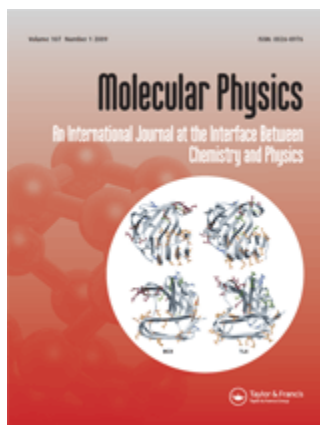
**HAL Id: hal-00513124**

**<https://hal.science/hal-00513124>**

Submitted on 1 Sep 2010

**HAL** is a multi-disciplinary open access archive for the deposit and dissemination of scientific research documents, whether they are published or not. The documents may come from teaching and research institutions in France or abroad, or from public or private research centers.

L'archive ouverte pluridisciplinaire **HAL**, est destinée au dépôt et à la diffusion de documents scientifiques de niveau recherche, publiés ou non, émanant des établissements d'enseignement et de recherche français ou étrangers, des laboratoires publics ou privés.



**(SI) Applications of analytic and geometry concepts of the theory of Calculus of Variations to the Intrinsic Reaction Coordinate model**

Journal:	<i>Molecular Physics</i>
Manuscript ID:	TMPH-2007-0194
Manuscript Type:	Full Paper
Date Submitted by the Author:	15-Jan-2007
Complete List of Authors:	Bofill, Josep Aguilar-Mogas, Antoni; Universitat de Barcelona Giménez, Xavier; Universitat de Barcelona Crehuet, Ramon; Institut de Investigacions Químiques i Ambientals de Barcelona
Keywords:	Reaction Path, Intrinsic Reaction Coordinate, Weierstrass E-function, Hamilton-Jacobi Equation, Monge Cone



# Applications of analytic and geometry concepts of the theory of Calculus of Variations to the Intrinsic Reaction

## Coordinate model\*

**Antoni Aguilar-Mogas<sup>†</sup>, Ramon Crehuet<sup>#</sup>, Xavier Giménez<sup>†</sup> and Josep Maria  
Bofill<sup>‡</sup>**

*<sup>†</sup>Departament de Química Física i Centre especial de Recerca en Química Teòrica,  
Universitat de Barcelona i Parc Científic de Barcelona, Martí i Franquès 1, 08028  
Barcelona, Spain.*

*<sup>‡</sup>Departament de Química Orgànica i Centre especial de Recerca en Química  
Teòrica, Universitat de Barcelona i Parc Científic de Barcelona, Martí i Franquès 1,  
08028 Barcelona, Spain.*

*<sup>#</sup>Departament de Química Orgànica Biològica, Institut de Investigacions Químiques i  
Ambientals de Barcelona, IIQAB-CSIC, Jordi Girona 18, 08034 Barcelona,  
Catalonia, Spain.*

A mathematical analysis of several algorithms, for the integration of the differential equation associated to the Intrinsic Reaction Coordinate path, is performed. This analysis starts showing that the Intrinsic Reaction Coordinate path can be derived from a variational problem, so that it has the properties of an extremal curve. Then, one may borrow the mathematical methods for the integration of extremal curves, to formulate new algorithms for the integration of the Intrinsic Reaction Coordinate path. One may use as well this theoretical framework, to recast recently formulated algorithms based on direct minimization of an arbitrary curve, such as the Nudged Elastic Band Method or String Method. In this view a new algorithm is proposed. Finally, the theory of broken extremals is used to analyze an Intrinsic Reaction Coordinate path possessing a valley ridge inflection point.

1  
2  
3  
4  
5  
6  
7  
8  
9  
10  
11  
12  
13  
14  
15  
16  
17  
18  
19  
20  
21  
22  
23  
24  
25  
26  
27  
28  
29  
30  
31  
32  
33  
34  
35  
36  
37  
38  
39  
40  
41  
42  
43  
44  
45  
46  
47  
48  
49  
50  
51  
52  
53  
54  
55  
56  
57  
58  
59  
60

*Keywords:* Reaction Path; Intrinsic Reaction Coordinate; Weierstrass  $E$ -function;  
Hamilton-Jacobi Equation; Monge Cone; Valley-Ridge-Inflection Point

\* Dedicated in honor to Professor Peter Pulay in his 65<sup>th</sup> birthday.

For Peer Review Only

## 1. INTRODUCTION

The development and applications of the concept of force and force constants in theoretical chemistry are one of the most important contributions of Professor Peter Pulay to this field [1, 2, 3, 4]. The use of forces or, equivalently, energy gradients, opened the possibility to explore the potential energy surfaces (PES) associated to chemical systems. In the early days, the explorations of the PES merely consisted in locating minima and first order saddle points, the latter corresponding to transition state structures. Even though this starting strategy was fairly simple, it already triggered, in both theoretical and applied chemistry communities, a major breakthrough, since this new tool made it easier to understand the structure of chemical systems. An important achievement in the development of model PESs, associated to chemical systems, was the introduction of the concept of reaction path (RP) or minimum energy path (MEP) by Fukui [5] as a way to describe in geometrical terms the chemical evolution from reactants to products. The importance of the RP concept was evidenced by the fast, continued development of powerful sets of algebraic, as well as computational, algorithms to locate the RP on a PES. Most algorithms use the gradients as a basic quantity. In this article we center our attention on a special form of RP or MEP, which will be analyzed from a specific mathematical framework.

From a strictly mathematical point of view, a RP is a curve line in the coordinate space connecting two minima through a first order saddle point (FOSP). The RP description of a chemical transformation is strictly geometrical, rigorously speaking, since it neglects the contribution of the kinetic energy stored in the nuclei. However, it is possible to provide RP-based methods to describe the temporal evolution of the reactive process, i.e. the dynamics. Actually, it is well known that the RP corresponds to a dynamic trajectory for an average of reactive collisions [6]. Miller, Handy and Adams followed this idea to formulate a reaction path Hamiltonian (RPH) [7, 8, 9], where the RP was used as a distinguished coordinate, the remaining coordinates being described by a Taylor expansion up to second order. Some of the present authors went further, and considered running the dynamics strictly on the RP. It may be shown that, within this restricted molecular motion, one should recover important classical and quantum dynamics effects [10]. On another hand, statistical

theories of reaction rates, such as the well-known Transition State Theory, along with their corresponding variational versions, are based on the RP model [11].

At first glance, it is a secondary matter of interest, which type of curve connects the FOSP and the minima of the PES associated to reactants and products. This may be the reason why a variety of RP definitions exists. The different definitions of RP correspond to different curve lines on the PES, and the parameterization of these lines,  $t$ , is the reaction coordinate. Using the mathematical language, if  $\mathbf{q}$  is the coordinate vector of dimension  $N$ , then the RP is represented as  $\mathbf{q}(t)$ . Very often the parameter arc-length of the curve,  $s$ , is taken as the reaction coordinate. Generally, one assumes that the MEP is the steepest descent (SD) curve connecting the minima of the PES associated to reactants and products from FOSP. This particular SD curve in mass weighted coordinates is known as Intrinsic Reaction Coordinate (IRC). At each point of the SD curve, their normalized tangent vector is equal to the normalized gradient vector,  $\mathbf{g}(\mathbf{q}) = \nabla_{\mathbf{q}} V(\mathbf{q})$ , of the PES,  $V(\mathbf{q})$ , at this point  $\mathbf{q}$ ,

$$\mathbf{t}(\mathbf{q}) = \left. \frac{d\mathbf{q}(s')}{ds'} \right|_{s'=s} = \frac{\mathbf{g}(\mathbf{q})}{\sqrt{(\mathbf{g}(\mathbf{q}))^T (\mathbf{g}(\mathbf{q}))}} \quad (1)$$

where,  $\mathbf{g}(\mathbf{q})$  and  $\mathbf{t}(\mathbf{q})$  are the gradient vector and the normalized tangent vector evaluated at the point of the curve,  $\mathbf{q} = \mathbf{q}(s)$ , respectively. The vector,  $\nabla_{\mathbf{q}}$ , is defined as,  $\nabla_{\mathbf{q}}^T = (\partial / \partial q_1, \dots, \partial / \partial q_N)$ , being  $q_i$  the element  $i$  of the vector  $\mathbf{q}$ . The superscript  $T$  means transposed. According to the autonomous differential equation (1), the SD paths and specifically the IRC curve are orthogonal curves to the contour lines  $V(\mathbf{q}) = \text{const}$  at each point of the curve. These contour lines are called equipotential curves or level curves of the PES. As an important consequence, the IRC path does not take into account the character of the curvature of each equipotential curve of the PES, which is transverse orthogonally by this path. Given a starting point, equation (1) determines one and only one SD curve, and this type of curves never bifurcates except at the stationary points of the PES,  $\mathbf{g}(\mathbf{q}) = \nabla_{\mathbf{q}} V(\mathbf{q}) = \mathbf{0}$ . In other words, except for the stationary points, one and only one SD curve runs through each point of the PES. From a mathematical point of view, the latter means that the solution of equation (1) is unique at each non-stationary point of the PES, or in other words, each SD curve is imbedded in the PES, which means that in the neighborhood of the projection of the SD curve in the  $\mathbf{q}$ -space, the PES,  $V$ , is a single valued, twice continuously

1  
2  
3 differentiable function with respect to  $\mathbf{q}$ . Finally, as noted several times, when in the  
4 evolution of an IRC path, at a point of this curve, the character of the curvature of the  
5 equipotential curve-lines of the PES changes from convex form to concave or ridge  
6 form, then after this point the IRC is not a real RP. In the latter assertion it is  
7 implicitly assumed that the true RP is a pathway connecting reactants and products  
8 through a valley floor. This behavior is a consequence of the fact that the IRC does  
9 not bifurcate. Due to the continuous way in the change of the curvatures of the levels  
10 of a PES, when a IRC evolves orthogonally through this set of levels, then a point of  
11 this IRC curve exists where the path transverses orthogonally a level with null  
12 curvature, this point is known as valley ridge inflection point (VRI). Notice that VRI  
13 points are inherent of the actual PES, not to the curve and we emphasize that IRC  
14 does not bifurcate at VRI points [12].

15  
16  
17  
18  
19  
20  
21  
22  
23  
24  
25  
26  
27  
28  
29  
30  
31  
32  
33  
34  
35  
36  
37  
38  
39  
40  
41  
42  
43  
44  
45  
46  
47  
48  
49  
50  
51  
52  
53  
54  
55  
56  
57  
58  
59  
60  
The parallelism between the SD paths and specifically the IRC curve and the  
Hamilton-Jacobi theory of the calculus of variations is evident if one considers the  
basic and complete picture of this mathematical theory. This complete picture merely  
consists in a relation between the curves and the contour lines of a surface, the surface  
where the curves are imbedded. These curves transverse in some way the set of  
contour lines and never are tangent to them. In the present case the curves are the SD  
lines, specifically the IRC, and the contour lines of a surface are the equipotential  
curves of PES under consideration. As noted in references [13, 14] this relation  
permits analyzing the IRC model using the theory of the Calculus of Variations (CV).  
In other words, the theory of Hamilton-Jacobi of the first order non-linear partial  
differential equations is closely connected with the theory of CV and permits  
analyzing the IRC curve model from this point of view [15]. In this way if the IRC  
curve is an extremal curve of some variational problem, then we can use the theory of  
Hamilton-Jacobi to integrate this type of curve. The integration of a partial  
differential equation is usually a problem more difficult than that of a system of  
ordinary differential equations. The Hamilton-Jacobi theory achieves an important  
success showing that this relation between these two classes of differential equations  
may be reversed. Many problems from the CV result in a system of ordinary  
differential equations and these equations may be difficult to integrate by normal  
methods, while the corresponding partial differential equation is easily solvable.  
When the complete integral that satisfies the partial differential equation of the  
corresponding variational problem is known then one solves the associated system of

1  
2  
3  
4  
5  
6  
7  
8  
9  
10  
11  
12  
13  
14  
15  
16  
17  
18  
19  
20  
21  
22  
23  
24  
25  
26  
27  
28  
29  
30  
31  
32  
33  
34  
35  
36  
37  
38  
39  
40  
41  
42  
43  
44  
45  
46  
47  
48  
49  
50  
51  
52  
53  
54  
55  
56  
57  
58  
59  
60

characteristic differential equations by differentiation and elimination. This procedure can be formulated in a simple way by using the envelope theory. In addition, the first order non-linear partial differential equation that appears in the CV can be solved through the construction of the Monge cone, which is build from the Monge differential equation. In fact it can be shown that the first order non-linear partial differential equation and Monge differential equation are dual to each other in the sense of projective geometry. The solutions of the Monge equation are curves such that at each point are tangent to a characteristic curve, the curve solution of the first order non-linear partial differential equation, which in turn is related with the extremal curve of the variational problem under consideration [15]. Since the IRC curve model becomes an extremal curve of a variational problem [14, 16], in this article we analyze the existing methods to integrate this type of curve from the above point of view based on the Monge cone construction.

More recently, an alternative way to locate the IRC curve in the PES has been proposed consisting in the minimization of a curve integral called the nudged elastic band method (NEB) or string method (SM). The integrand function is the square norm of the normal force of an arbitrary curve imbedded in the PES. The integral runs over the domain where the arbitrary curve is defined [17, 18, 19, 20, 21, 22]. The integral curve just defined is intimately related with the Weierstrass excess or error function that appears in the set of necessary conditions such that any extremal curve should satisfy to ensure its minimization (maximization) character of the functional integral of the variational problem under study. This relation has been analyzed recently by Crehuet and Bofill [14], however in this article will we study it in more detail from a strict mathematical point of view and a new algorithm will also be proposed.

Finally, the IRC curve passing trough a VRI, which in fact connects two minima of the PES through two consecutive FOSP's is analyzed as a broken extremal curve, a curve that possesses a corner.

## 2. THE NATURE OF THE INTEGRATION TECHNIQUES OF THE CALCULUS OF VARIATIONS AND ITS RELATION WITH THE



## INTEGRATION METHODS OF THE DIFFERENTIAL EQUATION CORRESPONDING TO THE INTRINSIC REACTION COORDINATE PATH

### 2.A) Algorithms based on the Theory of Monge Cone and Characteristic Curves: the Hamilton-Jacobi partial differential equation

The SD curve connecting the points of the PES,  $\mathbf{q}_R$  and  $\mathbf{q}$ , being  $\mathbf{q}_R$  a fixed point while  $\mathbf{q}$  is a variable point, is an extremal curve of the variational problem [14, 16],

$$\Delta V_{R \rightarrow q}(\mathbf{q}) = \int_{t_0}^t L(\mathbf{q}, d\mathbf{q}/dt) dt = \int_{t_0}^t \sqrt{\mathbf{g}^T \mathbf{g}} \sqrt{(d\mathbf{q}/dt)^T (d\mathbf{q}/dt)} dt \quad (2)$$

where  $t$  is the parameter that characterizes the curve. This result means that if a curve starting at the point  $\mathbf{q}_R$  and propagating through the PES according to the “speed law or continuous slowness model”,  $v(\mathbf{q}(t)) = [(\mathbf{g}(\mathbf{q}(t)))^T \mathbf{g}(\mathbf{q}(t))]^{1/2}$ , arrives at the point  $\mathbf{q} = \mathbf{q}(t)$ , traveling by extremalization of the potential energy variation,  $\Delta V_{R \rightarrow q}(\mathbf{q})$ , as defined in equation (2), then this curve is a SD path. It can be shown that this extremal curve possesses character minimum, which means that any other type of path connecting the points  $\mathbf{q}_R$  and  $\mathbf{q}$ , increases the value of the function,  $\Delta V_{R \rightarrow q}(\mathbf{q})$ , as defined in equation (2), with respect to the value obtained if this line integral is evaluated with the corresponding SD curve, connecting these two points [14]. The resulting value of the integral (2) evaluated on an extremal curve, SD line, will be denoted by  $J_R(\mathbf{q})$ . Notice that  $J_R(\mathbf{q})$  is the stationary value of  $\Delta V_{R \rightarrow q}(\mathbf{q})$ , the value of integral (2) evaluated on the SD curve, an extremal curve, joining the points  $\mathbf{q}_R$  and  $\mathbf{q}$ . This function is called geodetic distance between the points  $\mathbf{q}_R$  and  $\mathbf{q}$ , which means that the present variational problem can be seen as a generalization of the problem of finding the shortest curve between two points in space.

The integrand,  $L(\mathbf{q}, d\mathbf{q}/dt)$ , that appears in equation (2) is a homogeneous function of degree one with respect to the argument,  $d\mathbf{q}/dt$ , because it satisfies the relation,  $L(\mathbf{q}, d\mathbf{q}/dt) = (d\mathbf{q}/dt)^T [\nabla_{d\mathbf{q}/dt} L(\mathbf{q}, d\mathbf{q}/dt)]$ . Substituting this relation in equation (2) and assuming that the integral is evaluated on a SD curve, we obtain the next relation,

$$J_R(\mathbf{q}) = \int_{t_0}^t L(\mathbf{q}, d\mathbf{q}/dt) dt = \int_{\mathbf{q}_R}^{\mathbf{q}} [\nabla_{d\mathbf{q}/dt} L(\mathbf{q}, d\mathbf{q}/dt)]^T d\mathbf{q} \quad (3)$$

The last integral of expression (3), permits both, to consider the geodetic distance,  $J_R(\mathbf{q})$ , as a line integral of a total differential, independent of the path of integration, and to obtain the corresponding expression for the derivatives. This is so because for this function  $J_R(\mathbf{q})$  of the position  $\mathbf{q}$ , the equation

$$\begin{aligned}
 J_R(\mathbf{q}) &= \int_{\mathbf{q}_R}^{\mathbf{q}} (\nabla_{\mathbf{q}} J_R)_{\mathbf{q}=\mathbf{q}_C}^T d\mathbf{q}_C = \int_{t_0}^t (\nabla_{\mathbf{q}} J_R)_{\mathbf{q}=\mathbf{q}_C}^T (d\mathbf{q}_C/dt') dt' = \\
 & \int_{t_0}^t (\nabla_{\mathbf{q}} J_R)_{\mathbf{q}=\mathbf{q}'}^T (d\mathbf{q}'/dt') dt' = \int_{t_0}^t [\nabla_{d\mathbf{q}'/dt'} L(\mathbf{q}', d\mathbf{q}'/dt')]^T (d\mathbf{q}'/dt') dt' = \quad (4) \\
 & \int_{t_0}^t L(\mathbf{q}', d\mathbf{q}'/dt') dt'
 \end{aligned}$$

holds, where in the first two integrals the curve of integration between the points  $\mathbf{q}_R$  and  $\mathbf{q}$  is arbitrary with tangent,  $d\mathbf{q}_C/dt$  at the point  $\mathbf{q}_C$  of this curve, and the last three integrals are evaluated on the corresponding SD curve, where the symbols,  $\mathbf{q}'$  and  $d\mathbf{q}'/dt'$ , denote position and tangent vectors, respectively, of this SD curve connecting the points  $\mathbf{q}_R$  and  $\mathbf{q}$ . Notice again that the last line integral of equation (4) is evaluated on the SD curve connecting the points  $\mathbf{q}_R$  and  $\mathbf{q}$  and only in this case its value coincides with the line integral of the total differential form evaluated on a curve joining these two points. The simple form of this integral line is that defined in the first integral of equation (4). From the expressions (2) and (4) we obtain the derivative of  $J_R(\mathbf{q})$  with respect to  $\mathbf{q}$  at the point  $\mathbf{q}$ ,

$$\nabla_{\mathbf{q}} J_R(\mathbf{q}) = \nabla_{d\mathbf{q}/dt} L(\mathbf{q}, d\mathbf{q}/dt) = v(\mathbf{q}) \frac{d\mathbf{q}/dt}{\sqrt{(d\mathbf{q}/dt)^T (d\mathbf{q}/dt)}} \quad (5)$$

Multiplying equation (5) from the left by,  $[\nabla_{\mathbf{q}} J_R(\mathbf{q})]^T$ , we obtain the partial differential equation,

$$\frac{[\nabla_{\mathbf{q}} J_R(\mathbf{q})]^T [\nabla_{\mathbf{q}} J_R(\mathbf{q})]}{v^2(\mathbf{q})} - 1 = 0 \quad (6)$$

which is the *Hamilton-Jacobi equation or eiconal equation* for the geodetic distance,  $J_R$ , defined in equation (4), as a function of the end point  $\mathbf{q}$  [14]. The equation (6) is a first-order non-linear partial differential equation of the type,  $F(\mathbf{q}, \nabla_{\mathbf{q}} J_R) = 0$ , where both, the parameter  $t$  and  $J_R$  do not appear explicitly.

Now, we describe a method to solve the eiconal equation (6), which consists in finding a curve such that at each point of this curve the equation is satisfied [15]. Since this eiconal equation is a function of  $N$  independent variables, then from a

geometrical point of view, the solution of this equation,  $J_R(\mathbf{q})$ , is interpreted as a surface, the so-called integral surface in the  $\mathbf{q}$ ,  $J_R$ -space. Now, we assume that  $F(\mathbf{q}, \nabla_{\mathbf{q}}J_R)$  is continuous function with continuous first derivatives with respect to both types of arguments, namely,  $\mathbf{q}$  and  $\nabla_{\mathbf{q}}J_R = \mathbf{p}$ , in the region under consideration. In addition should be satisfied that  $[\nabla_{\mathbf{q}}J_R(\mathbf{q})]^T[\nabla_{\mathbf{q}}J_R(\mathbf{q})] \neq 0$ . From a geometrical point of view the equation (6) can be seen as follows, at any point  $(\mathbf{q}, J_R(\mathbf{q}))$ , the direction coefficients,  $\nabla_{\mathbf{q}}J_R(\mathbf{q})$ , of the plane tangent to an integral surface,  $J_R$ , in the  $\mathbf{q}$ ,  $J_R$ -space satisfies the equality,  $F(\mathbf{q}, \nabla_{\mathbf{q}}J_R) = 0$ . Since this equation is non linear in the  $\nabla_{\mathbf{q}}J_R(\mathbf{q})$  vector, then the possible tangent planes form a  $N-1$  parameter family enveloping a conical surface with the point  $(\mathbf{q}, J_R(\mathbf{q}))$  as a vertex. This conical surface is called the Monge cone. Notice that we are referring to a conical surface in the small. In this way the Hamilton-Jacobi equation (6) assigns a Monge cone to each point  $(\mathbf{q}, J_R(\mathbf{q}))$  in the domain under study. With these considerations, the problem of integrating the eiconal equation (6) consists in finding surfaces such that at each point are tangent to the corresponding cone. Now we represent the Monge cone,  $F(\mathbf{q}, \nabla_{\mathbf{q}}J_R) = 0$ , parametrically by taking the direction coefficients of the tangent plane enveloping it as a functions of a parameter  $\tau$ ,  $\nabla_{\mathbf{q}}J_R(\mathbf{q}, \tau)$ . A generating line of the Monge cone is the curve line resulting from the intersection of the tangent planes with parameters,  $\tau$ , and  $\tau + \varepsilon$ , respectively, as  $\varepsilon \rightarrow 0$ . This fact permits representing the Monge cone through a relation for their corresponding generating curve-lines instead of their relation through the tangent planes. For a given generating curve-line, the set of points of this curve,  $(\mathbf{q}, J_R(\mathbf{q}))$ , characterized by the parameter  $t$ , and taking into account that a point of this curve is the vertex of the cone, then the curve satisfies the set of equations,

$$\frac{dJ_R}{dt} = [\nabla_{\mathbf{q}}J_R(\mathbf{q}, \tau)]^T \frac{d\mathbf{q}}{dt} \quad (7.a)$$

$$0 = \left[ \frac{d}{d\tau} \nabla_{\mathbf{q}}J_R(\mathbf{q}, \tau) \right]^T \frac{d\mathbf{q}}{dt} \quad (7.b)$$

If we differentiate the equation  $F(\mathbf{q}, \nabla_{\mathbf{q}}J_R) = 0$  with respect to  $\tau$  we get,

$$\left[ \frac{d}{d\tau} \nabla_{\mathbf{q}}J_R(\mathbf{q}, \tau) \right]^T [\nabla_{\mathbf{p}}F(\mathbf{q}, \nabla_{\mathbf{q}}J_R)] = 0 \quad (8)$$

By comparing equations (7) and (8) we have the relations

$$\frac{d\mathbf{q}}{dt} = \nabla_{\mathbf{p}}F(\mathbf{q}, \nabla_{\mathbf{q}}J_R) \quad (9.a)$$

$$\frac{dJ_R}{dt} = [\nabla_{\mathbf{q}} J_R]^T [\nabla_{\mathbf{p}} F(\mathbf{q}, \nabla_{\mathbf{q}} J_R)] \quad (9.b)$$

The equations (9) are a representation of the Monge cone corresponding to the Hamilton-Jacobi equation (6). These relations of the generating lines of the Monge cone are called characteristic directions, and there is a one-parameter family of directions at each point. The curves possessing at each point a characteristic direction or characteristic tangent, are known as Monge curves. The differential equation (9.b) is called the strip condition. Notice that the functions,  $\mathbf{q}(t)$ ,  $J_R(\mathbf{q}(t))$ , and  $\nabla_{\mathbf{q}} J_R(\mathbf{q}(t))$ , define both a field of curves and a plane tangent to each curve at every point. This set of functions is called a strip. For this  $2N + 1$  functions of  $t$  we have an undetermined system, since we have  $N + 1$  system of ordinary differential equations (9) plus the equation (6). Now we make the following reasoning, since the integral surface  $J_R(\mathbf{q})$  at every point is tangent to the Monge cone, then it possesses a characteristic direction or characteristic tangent and as a consequence a Monge curve. The field of tangents or characteristic directions defines a set of Monge curves and they are the integral curves on the integral surface  $J_R(\mathbf{q})$ . As a consequence we can say that the Monge curve is imbedded in an integral surface and vice versa the field of Monge curves generates the corresponding integral surface and this fact permits deriving the  $N$  system of ordinary differential equations for the  $\nabla_{\mathbf{q}} J_R(\mathbf{q}(t))$  argument. Now if we differentiate the Hamilton-Jacobi equation (6) with respect to  $\mathbf{q}$  we get the relation

$$[\nabla_{\mathbf{q}} \nabla_{\mathbf{q}}^T J_R(\mathbf{q})] \nabla_{\mathbf{p}} F(\mathbf{q}, \nabla_{\mathbf{q}} J_R) + \nabla_{\mathbf{q}} F(\mathbf{q}, \nabla_{\mathbf{q}} J_R) = \mathbf{0} \quad (10)$$

Since the Monge curve with  $t$  as a parameter that characterizes this curve, satisfies equation (9.a) then equation (10) can be rewritten as

$$\frac{d}{dt} [\nabla_{\mathbf{q}} J_R(\mathbf{q})] + \nabla_{\mathbf{q}} F(\mathbf{q}, \nabla_{\mathbf{q}} J_R) = \mathbf{0} \quad (11)$$

Finally, if we assume that the Monge curve is imbedded in an integral surface, then the functions  $\mathbf{q}(t)$ ,  $J_R(\mathbf{q}(t))$ , and  $\nabla_{\mathbf{q}} J_R(\mathbf{q}(t)) = \mathbf{p}$ , along this curve satisfy the system of  $2N + 1$  ordinary differential equations

$$\frac{d\mathbf{q}}{dt} = \nabla_{\mathbf{p}} F(\mathbf{q}, \nabla_{\mathbf{q}} J_R) \quad (12.a)$$

$$\frac{dJ_R(\mathbf{q})}{dt} = [\nabla_{\mathbf{q}} J_R]^T [\nabla_{\mathbf{p}} F(\mathbf{q}, \nabla_{\mathbf{q}} J_R)] \quad (12.b)$$

$$\frac{d}{dt} [\nabla_{\mathbf{q}} J_R(\mathbf{q})] = -\nabla_{\mathbf{q}} F(\mathbf{q}, \nabla_{\mathbf{q}} J_R) \quad (12.c)$$

Equations (12) are the characteristic system of differential equations corresponding to the Hamilton-Jacobi equation (6). According to the definitions used in the theory of partial differential equations, we say that every solution of the system of equations (12) which also satisfies the equation (6),  $F(\mathbf{q}, \nabla_{\mathbf{q}}J_R) = 0$ , is called a characteristic strip, and the curve,  $\mathbf{q}(t)$ ,  $J_R(\mathbf{q}(t))$  bearing such a strip is called a characteristic curve. These strips form a  $2N - 1$  parameter family. The extremal curve of the variational problem (2) is obtained by the projection of the characteristic curve from the  $\mathbf{q}$ ,  $J_R$ -space to the  $\mathbf{q}$ -subspace. For the present problem equations (12) take the form

$$\frac{d\mathbf{q}}{dt} = \nabla_{\mathbf{q}}J_R(\mathbf{q}) \quad (13.a)$$

$$\frac{dJ_R(\mathbf{q})}{dt} = [\nabla_{\mathbf{q}}J_R(\mathbf{q})]^T [\nabla_{\mathbf{q}}J_R(\mathbf{q})] \quad (13.b)$$

$$\frac{d}{dt} [\nabla_{\mathbf{q}}J_R(\mathbf{q})] = \frac{1}{2} \nabla_{\mathbf{q}}v^2(\mathbf{q}) \quad (13.c)$$

where,  $\nabla_{\mathbf{q}}J_R = \mathbf{p} = \mathbf{g}(\mathbf{q})$ , is the gradient vector evaluated at the point of the curve,  $\mathbf{q} = \mathbf{q}(t)$ , of the SD curve with initial point,  $\mathbf{q}_R = \mathbf{q}(t_0)$  and initial  $\mathbf{p}_R$  vector. From the Theory of CV just exposed, the above results are the mathematical background of the important set of methods used to integrate the IRC curve [23, 7, 24, 25, 26, 27, 28, 29, 30, 31, 32, 33, 34, 35, 36, 37, 38, 39]. Recently, an algorithm based on the simultaneous integration of the above set of differential equations (13) to obtain the IRC curve has been proposed, doing the integration through the Runge-Kutta-Fehlberg technique [16]. In the Appendix A we give a proof of the above assertion where the well known integrated form of equations (13) for a quadratic PES are derived by using the Jacobi method based in the construction of an envelope [15].

Finally, we conclude this subsection emphasizing, for posteriors purposes, that the solution of the eiconal equation (6),  $J_R(\mathbf{q})$ , defines a field of extremal curves, SD curves, all starting from the  $\mathbf{q}_R$  point a stationary point character minimum of the PES. As a consequence, each SD curve, or extremal curve, of this field cuts transversally the equipotential curves of the PES, each one at a different point. The IRC curve is an SD extremal curve imbedded in this field of extremals curves.

## 2.B) Algorithm based on the Theory of Second Variation: minimization of the line integral of the Weierstrass $E$ -Function

The concept of close neighborhood is important in the analysis and solutions of the variational problems in the small [40, 41]. Let us considered a curve,  $\mathbf{q}(t)$ , with continuous tangent,  $d\mathbf{q}(t)/dt$ . This curve is in the present case a SD curve. The line elements of this curve are determined by the  $2N + 1$  numbers, namely,  $(t, \mathbf{q}, d\mathbf{q}/dt)$ , which are points of a  $2N + 1$ -dimensional space. Now, we consider a second curve,  $\mathbf{q}_C(t)$ , defined in the same interval of  $t$ . This curve is called a “variation” of the  $\mathbf{q}(t)$  curve, or a “comparison curve”. The curve  $\mathbf{q}_C(t)$  is continuous in the interval of  $t$  but only piecewise continuous differentiable, that is, may be possesses a finite number of corners. The comparison curve,  $\mathbf{q}_C(t)$ , belongs to a close neighborhood,  $(\varepsilon_1, \varepsilon_2)$ , of the curve  $\mathbf{q}(t)$  if in the desired interval of  $t$ , the relations  $|\mathbf{q}_i(t) - \mathbf{q}_{Ci}(t)| < \varepsilon_1$  and  $|d\mathbf{q}_i(t)/dt - d\mathbf{q}_{Ci}(t)/dt| < \varepsilon_2$ , for  $\forall i = 1, \dots, N$ , hold. The latter relation is only applicable at the points of  $t$  where the tangent vector,  $d\mathbf{q}_C(t)/dt$ , exists.

Now we assume that the functional,  $L(\mathbf{q}, d\mathbf{q}/dt)$ , given in expression (2), is defined in the  $2N$ -dimensional space and in addition is a twice continuously differentiable function of the  $\mathbf{q}$  and  $d\mathbf{q}(t)/dt$ , variables. The vector,  $d\mathbf{q}(t)/dt$ , is the tangent vector of the extremal curve, the SD curve. If we expand in Taylor series the functional,  $L(\mathbf{q}, d\mathbf{q}/dt)$ , in powers of  $(d\mathbf{q}_C(t)/dt - d\mathbf{q}(t)/dt)$  and truncate the series after the linear terms, and taking into account that  $L(\mathbf{q}, d\mathbf{q}/dt)$  is a homogeneous functional of degree one with respect to,  $d\mathbf{q}/dt$ , we obtain

$$\begin{aligned} L(\mathbf{q}, d\mathbf{q}_C/dt) &= L(\mathbf{q}, d\mathbf{q}/dt) + (d\mathbf{q}_C/dt - d\mathbf{q}/dt)^T \left[ \nabla_{d\mathbf{q}/dt} L(\mathbf{q}, d\mathbf{q}/dt) \right]_{d\mathbf{q}/dt} \\ &+ E(\mathbf{q}, d\mathbf{q}/dt, d\mathbf{q}_C/dt) \\ &= (d\mathbf{q}_C/dt)^T \left[ \nabla_{d\mathbf{q}/dt} L(\mathbf{q}, d\mathbf{q}/dt) \right]_{d\mathbf{q}/dt} + E(\mathbf{q}, d\mathbf{q}/dt, d\mathbf{q}_C/dt) \end{aligned} \quad (14)$$

The remainder,  $E(\mathbf{q}, d\mathbf{q}/dt, d\mathbf{q}_C/dt)$ , is the Weierstrass  $E$ -function also known as excess or error function [40, 41]. This Weierstrass  $E$ -function vanishes only when the vector  $(d\mathbf{q}_C(t)/dt - d\mathbf{q}(t)/dt) = \mathbf{0}$ , that is when the curve with tangent  $d\mathbf{q}_C(t)/dt$  coincides with the extremal curve, in the present case the SD curve. The remainder takes the following explicit general form,

$$\begin{aligned} E(\mathbf{q}, d\mathbf{q}/dt, d\mathbf{q}_C/dt) &= 1/2 (d\mathbf{q}_C/dt - d\mathbf{q}/dt)^T \\ &\times \left[ \nabla_{d\mathbf{q}/dt} \nabla_{d\mathbf{q}/dt}^T L(\mathbf{q}, d\mathbf{q}/dt) \right]_{d\mathbf{q}/dt = d\mathbf{q}/dt + \vartheta (d\mathbf{q}_C/dt - d\mathbf{q}/dt)} (d\mathbf{q}_C/dt - d\mathbf{q}/dt) \end{aligned} \quad (15)$$

where  $0 < \vartheta < 1$ . If we integrate equation (14) through the arbitrary path  $C$ , connecting the points  $\mathbf{q}_R = \mathbf{q}(t_0)$  and  $\mathbf{q}^* = \mathbf{q}(t)$ , which possesses piecewise continuous tangents and except in the corners, but if this arbitrary curve has corners, and the



inequality,  $|d\mathbf{q}_i(t)/dt - d\mathbf{q}_{Ci}(t)/dt| < \varepsilon_2$ , for  $\forall i = 1, \dots, N$ , in both cases holds, then after some rearrangements, we get

$$\int_{t_0}^t E(\mathbf{q}, d\mathbf{q}/dt', d\mathbf{q}_C/dt') dt' = \int_{t_0}^t L(\mathbf{q}, d\mathbf{q}_C/dt') dt' - J_R(\mathbf{q}^*) \quad (16)$$

In the derivation of expression (16) we have used that  $\nabla_{\mathbf{q}} J_R(\mathbf{q}) = [\nabla_{d\mathbf{q}/dt} L(\mathbf{q}, d\mathbf{q}/dt)]_{d\mathbf{q}/dt}$ , and the second equality of equation (4). Notice that in equation (16), the tangent vector,  $d\mathbf{q}/dt$ , is the tangent of the SD curve, the extremal curve,  $d\mathbf{q}/dt = \mathbf{g}(\mathbf{q})$ . The above equation (16) establishes the Weierstrass sufficient condition for an extremal curve to be strong relative minimum (maximum) for the functional integral like given in equation (2). Regarding the right hand side part of equation (16), we can say that the question about strong relative minimum (maximum) for the functional integral is reduced to a comparison of integrands alone. It can be shown that the Weierstrass sufficient condition is related to the second variation of the functional integral of expression (2) with respect to the function  $\mathbf{q}(t)$ . Using this condition, one assumes that the extremal curve under study can be imbedded in a field of extremal curves, in the present case a field of SD curves, as mentioned at the end of the previous subsection. If this is not possible then the second variation of the integral (2) cannot be expressed as a function of the Weierstrass  $E$ -function alone in the domain under consideration, and as a consequence, it is not correct to conclude whether an extremal curve is a strong relative minimum (maximum) taking into account the value of equation (16). We can always imbed an extremal curve, SD curve, in a field if the endpoints of the curve are not too far. A family of extremal curves starting from the point,  $\mathbf{q}_R = \mathbf{q}(t_0)$ , a stationary point character minimum of the PES, will constitute a field up to its envelope. In other words, if  $\mathbf{q}(t)$  is a SD curve starting at the  $\mathbf{q}_R$  point, the first point at which this extremal curve is intersected again by other neighboring SD curve of this field, is called the conjugate point of  $\mathbf{q}_R$ . The conjugate point is the intersection of the SD curve,  $\mathbf{q}(t)$ , with the envelope. If the conjugate point is the point  $\mathbf{q}(t_{CP})$ , then the necessary and sufficient conditions given by equation (16) can be applied only in the interval,  $t_0 \leq t < t_{CP}$  [40, 41]. It can be shown that the IRC curve, a SD curve connecting two stationary points character minimum of the PES through a first order saddle point, does not possess conjugate point, in all the interval [14]. We emphasize that all these conclusions are applied to a field of continuous extremal curves, SD curves, with continuous tangent at each point of the curve.

If the functional,  $L(\mathbf{q}, d\mathbf{q}/dt)$ , given in the expression (2) is substituted in equation (14), we obtain the Weierstrass  $E$ -function for the SD curve,

$$E(\mathbf{q}, \mathbf{g}, d\mathbf{q}_C/dt) = \left[ 1 - \frac{\mathbf{g}^T (d\mathbf{q}_C/dt)}{\sqrt{\mathbf{g}^T \mathbf{g}} \sqrt{(d\mathbf{q}_C/dt)^T (d\mathbf{q}_C/dt)}} \right] L(\mathbf{q}, d\mathbf{q}_C/dt) \quad (17)$$

According to equation (17), we can say that the Weierstrass  $E$ -function for the SD curve is always positive,  $E(\mathbf{q}, \mathbf{g}, d\mathbf{q}_C/dt) \geq 0$ , and in addition, using equation (16) we conclude that the SD curves are extremals of character minimum. In other words, the SD curves make minimum the integral line (2) with respect to other “comparison curves”, connecting the same end points,  $\mathbf{q}_R$ , and  $\mathbf{q}^*$ , in the given neighborhood.

The Weierstrass  $E$ -function can be interpreted geometrically in a very striking manner [41]. For this purpose, let us consider the surface defined by the equation,  $L(\mathbf{q}, d\mathbf{q}/dt) = 1$ , where the variable is the tangent vector,  $d\mathbf{q}/dt$ , while the argument,  $\mathbf{q}$ , represents the coordinates of the point at which the tangent vector space is defined. The functional,  $L(\mathbf{q}, d\mathbf{q}/dt)$ , is that given in equation (2). For any tangent vector,  $d\mathbf{q}_C/dt$ , issuing from the origin vector,  $d\mathbf{q}/dt = \mathbf{0}$ , we can find a positive number  $\xi$  such that  $L(\mathbf{q}, \xi d\mathbf{q}_C/dt) = 1$ , and this is possible because the functional  $L(\mathbf{q}, d\mathbf{q}/dt)$  is homogeneous of degree one with respect to the  $d\mathbf{q}/dt$  argument. Notice that  $\xi = [L(\mathbf{q}, d\mathbf{q}/dt)]^{-1}$ . Therefore, any tangent vector issuing from the origin vector  $\mathbf{0}$ , will intersect the surface,  $L(\mathbf{q}, d\mathbf{q}/dt) = 1$ , once and only once. This surface is known as the indicatrix. Now, let  $d\mathbf{q}/dt$  the tangent vector of the SD curve at the point  $\mathbf{q}$ , and  $d\mathbf{q}_{SD}/dt = \xi d\mathbf{q}/dt$ , a fixed point of the indicatrix, such that  $L(\mathbf{q}, d\mathbf{q}_{SD}/dt) = 1$ . The equation of the tangent plane to the indicatrix at this fixed point,  $d\mathbf{q}_{SD}/dt$ , is

$$(d\mathbf{q}'/dt - d\mathbf{q}_{SD}/dt)^T \left[ \nabla_{d\mathbf{q}/dt} L(\mathbf{q}, d\mathbf{q}/dt) \right]_{d\mathbf{q}/dt=d\mathbf{q}_{SD}/dt} = 0 \quad (18)$$

In equation (18), the arguments,  $\mathbf{q}$  and  $d\mathbf{q}_{SD}/dt$ , are fixed, while the argument,  $d\mathbf{q}'/dt$ , is the variable. Using both, that the functional  $L(\mathbf{q}, d\mathbf{q}/dt)$  is homogeneous and  $L(\mathbf{q}, d\mathbf{q}_{SD}/dt) = 1$ , equation (18) can be rewritten as

$$(d\mathbf{q}'/dt)^T \left[ \nabla_{d\mathbf{q}/dt} L(\mathbf{q}, d\mathbf{q}/dt) \right]_{d\mathbf{q}/dt=d\mathbf{q}_{SD}/dt} = 1 \quad (19)$$

Let  $d\mathbf{q}_C/dt$ , be tangent vector of the arbitrary curve  $C$  at the same point  $\mathbf{q}$ , and  $d\mathbf{q}'_C/dt = \xi' d\mathbf{q}_C/dt$ , be another fixed point of the indicatrix. Notice that  $\xi'$  is computed such that the equality,  $L(\mathbf{q}, d\mathbf{q}'_C/dt) = 1$ , is satisfied taking as the origin of  $d\mathbf{q}'_C/dt$  vector the  $\mathbf{0}$  vector. Starting at the point,  $d\mathbf{q}'_C/dt$ , we construct a vector parallel to the vector,  $d\mathbf{q}_{SD}/dt$ , such that it meets the tangent plane given in equation (19) at the



point,  $d\mathbf{q}'/dt$ . Thus the resulting constructed vector has components,  $\chi d\mathbf{q}_{SD}/dt$ , where  $\chi$  is a real number and takes the value zero when,  $d\mathbf{q}_{SD}/dt = d\mathbf{q}'_C/dt$ . Now we want to find an analytical expression for the  $\chi$  number. By the construction, the vector  $d\mathbf{q}'/dt$ , with origin at  $\mathbf{0}$  vector, has components,  $d\mathbf{q}'/dt = d\mathbf{q}'_C/dt + \chi d\mathbf{q}_{SD}/dt$ , and satisfies equation (19),

$$(d\mathbf{q}'_C/dt + \chi d\mathbf{q}_{SD}/dt)^T [\nabla_{d\mathbf{q}/dt} L(\mathbf{q}, d\mathbf{q}/dt)]_{d\mathbf{q}/dt=d\mathbf{q}_{SD}/dt} = 1 \quad (20)$$

After some rearrangements we obtain,

$$\begin{aligned} \chi &= 1 - \frac{\sqrt{\mathbf{g}^T \mathbf{g}} (d\mathbf{q}_{SD}/dt)^T (d\mathbf{q}_C/dt) \xi'}{\sqrt{(d\mathbf{q}_{SD}/dt)^T (d\mathbf{q}_{SD}/dt)} \sqrt{(d\mathbf{q}_C/dt)^T (d\mathbf{q}_C/dt)}} \\ &= 1 - \frac{(d\mathbf{q}_{SD}/dt)^T (d\mathbf{q}_C/dt)}{\sqrt{(d\mathbf{q}_{SD}/dt)^T (d\mathbf{q}_{SD}/dt)} \sqrt{(d\mathbf{q}_C/dt)^T (d\mathbf{q}_C/dt)}} \\ &= 1 - \frac{\mathbf{g}^T (d\mathbf{q}_C/dt)}{\sqrt{\mathbf{g}^T \mathbf{g}} \sqrt{(d\mathbf{q}_C/dt)^T (d\mathbf{q}_C/dt)}} = \frac{E(\mathbf{q}, \mathbf{g}, d\mathbf{q}_C/dt)}{L(\mathbf{q}, d\mathbf{q}_C/dt)} \end{aligned} \quad (21)$$

where we have used that the tangent of the SD curve is,  $d\mathbf{q}_{SD}/dt = \mathbf{g}$ . Expression (21) tells us that the Weierstrass  $E$ -function is the ratio or proportionality factor between the vectors,  $d\mathbf{q}_{SD}/dt$ , and  $d\mathbf{q}'/dt - d\mathbf{q}'_C/dt$ . This result is based on the Carathéodory's geometrical interpretation of the Weierstrass  $E$ -function [41]. In figure 1 we give a graphical scheme where all the above concepts are shown.

[Please insert figure 1 near here]

From the above geometrical point of view of the Weierstrass  $E$ -function we can reason in the following way, given an arbitrary curve  $C$  such that at point  $\mathbf{q}$  of this curve the tangent is  $d\mathbf{q}_C/dt$ , then we can find the SD curve passing through this point by minimization of the corresponding Weierstrass  $E$ -function of this point. If this procedure is applied to a whole curve connecting two given points, say  $\mathbf{q}_R$  and  $\mathbf{q}^*$ , then we obtain the SD curve connecting these points. It is assumed that the arbitrary  $C$  curve is imbedded in the field of the SD curves. Finally, if the points  $\mathbf{q}_R$  and  $\mathbf{q}^*$ , correspond to two stationary points of the PES with character minimum, associated to reactants and products respectively, then the located SD curve is the IRC curve. With this procedure, one achieves to make zero the integral of the left hand side part of equation (16), which means that the line integral evaluated on the converged curve is

equal to  $J_R(\mathbf{q}^*)$ , the value of the line integral (2) computed on the SD curve that connects the points  $\mathbf{q}_R$  and  $\mathbf{q}^*$ . To be clear we rewrite equation (16) as

$$\begin{aligned} \int_{t_0}^t E(\mathbf{q}, \mathbf{g}, d\mathbf{q}_C/dt') dt' &= \frac{1}{2} \int_{t_0}^t \left( 2 - \frac{2\mathbf{g}^T (d\mathbf{q}_C/dt')}{\sqrt{\mathbf{g}^T \mathbf{g}} \sqrt{(d\mathbf{q}_C/dt')^T (d\mathbf{q}_C/dt')}} \right) L(\mathbf{q}, d\mathbf{q}_C/dt') dt' \\ &= \frac{1}{2} \int_{t_0}^t \left( \frac{d\mathbf{q}_C/dt'}{\sqrt{(d\mathbf{q}_C/dt')^T (d\mathbf{q}_C/dt')}} - \frac{\mathbf{g}}{\sqrt{\mathbf{g}^T \mathbf{g}}} \right)^T \left( \frac{d\mathbf{q}_C/dt'}{\sqrt{(d\mathbf{q}_C/dt')^T (d\mathbf{q}_C/dt')}} - \frac{\mathbf{g}}{\sqrt{\mathbf{g}^T \mathbf{g}}} \right) L(\mathbf{q}, d\mathbf{q}_C/dt') dt' \end{aligned} \quad (22)$$

where equation (17) has been used. This expression is the basis of the algorithm to locate IRC curve on the PES proposed in reference [14]. Notice that the integral of equation (22) is zero if the normalized tangent vector of the arbitrary curve  $C$  at each point is parallel with respect to the normalized gradient vector at this point of the PES, or, what is the same, the component of this gradient vector in the orthogonal subspace of the tangent vector of this arbitrary curve  $C$  is equal to zero at each point of the curve,  $(\mathbf{g} - \mathbf{t}_C \mathbf{t}_C^T \mathbf{g}) = \mathbf{0}$ , being  $\mathbf{t}_C = (d\mathbf{q}_C/dt') / [(d\mathbf{q}_C/dt')^T (d\mathbf{q}_C/dt')]^{1/2}$ , the normalized tangent vector of the  $C$  curve at the point  $\mathbf{q}$ , and  $\mathbf{g} = \mathbf{g}(\mathbf{q})$ . The latter reasoning is the basis of the NEB and SM methods [17, 18, 19, 20, 21, 22] and also that proposed by Ayala and Schlegel [42] and shows clearly their connection with the statement that *the minimization until the zero value of the line integral of the Weierstrass E-function. The condition of zero value of the line integral of the Weierstrass E-function appears in the set of necessary and sufficient conditions of a curve to be an extremal curve, like the IRC path, ensuring that this curve gives the minimum value to the line integral (2) with respect to others "comparison curves"*.

Now we outline briefly an algorithm based on the direct minimization of the integral given in equation (22) to locate the IRC curve as discussed above.

1. Give a guess path,  $C$ , connecting the points  $\mathbf{q}_R$  and  $\mathbf{q}^*$ . The path  $C$  is represented by a polygonal curve and assumed to be in a close neighborhood of the desired IRC path. The points  $\mathbf{q}_R$  and  $\mathbf{q}^*$  are two stationary points of the PES with character minimum.
2. Compute at each vertex of the polygonal curve  $C$ , the Weierstrass  $E$ -function. The discretized expressions of both the Weierstrass  $E$ -function,  $E_{dis}(\mathbf{g}_\mu, \Delta\mathbf{q}_\mu)$ , and the integral given in equation (22) evaluated over the polygonal curve  $C$ , are

$$\begin{aligned}
& \sum_{\mu=1}^{\text{number of vertices}} E_{dis}(\mathbf{g}_\mu, \Delta \mathbf{q}_\mu) \sqrt{\Delta \mathbf{q}_\mu^T \Delta \mathbf{q}_\mu} \\
&= \sum_{\mu=1}^{\text{number of vertices}} \left( 1 - \frac{\mathbf{g}_\mu^T \Delta \mathbf{q}_\mu}{\sqrt{\mathbf{g}_\mu^T \mathbf{g}_\mu} \sqrt{\Delta \mathbf{q}_\mu^T \Delta \mathbf{q}_\mu}} \right) \sqrt{\mathbf{g}_\mu^T \mathbf{g}_\mu} \sqrt{\Delta \mathbf{q}_\mu^T \Delta \mathbf{q}_\mu} \\
&= \frac{1}{2} \sum_{\mu=1}^{\text{number of vertices}} \left( \frac{\Delta \mathbf{q}_\mu}{\sqrt{\Delta \mathbf{q}_\mu^T \Delta \mathbf{q}_\mu}} - \frac{\mathbf{g}_\mu}{\sqrt{\mathbf{g}_\mu^T \mathbf{g}_\mu}} \right)^T \left( \frac{\Delta \mathbf{q}_\mu}{\sqrt{\Delta \mathbf{q}_\mu^T \Delta \mathbf{q}_\mu}} - \frac{\mathbf{g}_\mu}{\sqrt{\mathbf{g}_\mu^T \mathbf{g}_\mu}} \right) \sqrt{\mathbf{g}_\mu^T \mathbf{g}_\mu} \sqrt{\Delta \mathbf{q}_\mu^T \Delta \mathbf{q}_\mu}
\end{aligned} \tag{23.a}$$

where  $\mathbf{g}_\mu = \mathbf{g}(\mathbf{q}_\mu)$  and  $\Delta \mathbf{q}_\mu = \mathbf{q}_{\mu+1} - \mathbf{q}_\mu$ . The index  $\mu$  runs over the number of vertices of the  $C$  polygonal curve, and each  $\mathbf{q}_\mu$  represents the position of each vertex. If the value of equation (23.a) is below a given threshold then the current  $C$  curve is the IRC curve joining the stationary points  $\mathbf{q}_R$  and  $\mathbf{q}^*$  in the PES.

3. At each vertex  $\mu$ , the derivative of the above expression (23.a) with respect to  $\mathbf{q}_\mu$  is computed according to the formula,

$$\begin{aligned}
& \nabla_{\mathbf{q}_\mu} \left( \sum_{v=1}^{\text{number of vertices}} E_{dis}(\mathbf{g}_v, \Delta \mathbf{q}_v) \sqrt{\Delta \mathbf{q}_v^T \Delta \mathbf{q}_v} \right) \\
&= \nabla_{\mathbf{q}_\mu} \left( E_{dis}(\mathbf{g}_\mu, \Delta \mathbf{q}_\mu) \sqrt{\Delta \mathbf{q}_\mu^T \Delta \mathbf{q}_\mu} + E_{dis}(\mathbf{g}_{\mu-1}, \Delta \mathbf{q}_{\mu-1}) \sqrt{\Delta \mathbf{q}_{\mu-1}^T \Delta \mathbf{q}_{\mu-1}} \right) \\
&= -\mathbf{H}_\mu \left( \frac{\Delta \mathbf{q}_\mu}{\sqrt{\Delta \mathbf{q}_\mu^T \Delta \mathbf{q}_\mu}} - \frac{\mathbf{g}_\mu}{\sqrt{\mathbf{g}_\mu^T \mathbf{g}_\mu}} \right) \sqrt{\Delta \mathbf{q}_\mu^T \Delta \mathbf{q}_\mu} - \left( \frac{\Delta \mathbf{q}_\mu}{\sqrt{\Delta \mathbf{q}_\mu^T \Delta \mathbf{q}_\mu}} - \frac{\mathbf{g}_\mu}{\sqrt{\mathbf{g}_\mu^T \mathbf{g}_\mu}} \right) \sqrt{\mathbf{g}_\mu^T \mathbf{g}_\mu} \\
&+ \left( \frac{\Delta \mathbf{q}_{\mu-1}}{\sqrt{\Delta \mathbf{q}_{\mu-1}^T \Delta \mathbf{q}_{\mu-1}}} - \frac{\mathbf{g}_{\mu-1}}{\sqrt{\mathbf{g}_{\mu-1}^T \mathbf{g}_{\mu-1}}} \right) \sqrt{\mathbf{g}_{\mu-1}^T \mathbf{g}_{\mu-1}} = \mathbf{e}_\mu
\end{aligned} \tag{23.b}$$

where,  $\mathbf{H}_\mu = \mathbf{H}(\mathbf{q}_\mu)$ , is the Hessian matrix evaluated at the point  $\mathbf{q}_\mu$ . The new point vertex,  $\mathbf{q}_{\mu'}$ , is found by minimization of the potential energy,  $V(\mathbf{q}_\mu)$ , in the direction given by vector of the equation (23.b),

$$V(\mathbf{q}_\mu + \mathbf{e}_\mu \alpha_\mu) = V(\mathbf{q}_\mu) + \mathbf{g}_\mu^T \mathbf{e}_\mu \alpha_\mu + 1/2 \mathbf{e}_\mu^T \mathbf{H}_\mu \mathbf{e}_\mu \alpha_\mu^2 \tag{23.c}$$

The minimization is stopped when both,  $V(\mathbf{q}_\mu) - V(\mathbf{q}_\mu + \mathbf{e}_\mu \alpha_\mu)$  and  $|\alpha_\mu|$ , satisfy some criteria. The trust radius technique is used to find the

appropriated minimization step [43]. Once  $\alpha_\mu$  is obtained the new vertex is computed through the equation,  $\mathbf{q}_\mu' = \mathbf{q}_\mu + \mathbf{e}_\mu \alpha_\mu$ .

4. If the new set of vertices,  $\{\mathbf{q}_\mu'\}_{\mu=1}^{\text{number of vertices}}$ , does not define a curve satisfying the requirements of regular curve then a parameterization of the curve is needed. After the parameterization is done, the new set of vertices define the new curve  $C'$ . Doing  $C' \rightarrow C$ , the process is started again at the step 2.

Now we comment the just outlined algorithm to find IRC curves, to justify the procedure with the explained mathematical elements of the theory of CV. The guess curve and the set of intermediate curves generated by the algorithm, labeled by  $C$ , are curves of the type “comparison curves” introduced in the first paragraph of the present subsection. The convergence criteria of step 2, is justified since this implies that at each vertex of the current  $C$  curve, the equality  $\Delta\tilde{\mathbf{q}}_\mu \Delta\tilde{\mathbf{q}}_\mu^T \Delta\tilde{\mathbf{q}}_\mu \cdot \tilde{\mathbf{g}}_\mu \tilde{\mathbf{g}}_\mu^T \tilde{\mathbf{g}}_\mu)^{1/2}$ , for  $\mu = 1, \dots, \text{number of vertices}$ , is satisfied which is nothing more than the discretized form of equation (1), the tangent equation of the IRC curve. In the sub arc of the current curve  $C$  such that the energy of the PES decreases according to the defined direction of the curve then the set of vectors,  $\Delta\tilde{\mathbf{q}}_\mu \Delta\tilde{\mathbf{q}}_\mu^T \Delta\tilde{\mathbf{q}}_\mu$ , associated to the vertices of this sub arc are changed of sign. The minimization of the PES at each vertex of the current curve, as explained in step 3, ensures that the procedure will not converge to a SD curve with conjugate points. As discussed above, the IRC curve is a SD curve free of conjugate points, otherwise the curve does not satisfy the set of sufficient conditions to minimize the integral (2) between the points  $\mathbf{q}_R$  and  $\mathbf{q}^*$ . A SD curve, connecting two points character minimum of the PES, possesses a conjugate point if a point of this curve is a stationary point with character of order higher than one [14]. Since stationary points of the PES with character of order higher than one possess values of  $V$  that are higher to the values of  $V$  of the corresponding stationary points with character first order (FOSP), then in order to satisfy the above requirement we force the minimization process at each vertex of the current discretized curve  $C$ , ensuring in this way that the curve does not possess a conjugate point. After the minimization is completed for all vertices of the current curve as required in step 3, maybe the resulting new set of vertices does not define a curve to be an admissible “comparison curve”. This is the reason of the last step 4. An admissible “comparison

curve” is a regular curve [40], which means that  $\mathbf{q}(t)$  is a single-valued function and the derivatives are well defined in the whole interval,  $t_0 \leq t \leq t_f$ , being,  $\mathbf{q}^* = \mathbf{q}(t_f)$ . For discretized curves, such as used in the present algorithm, this requirement is obeyed first, if the curve shows a monotonic increasing or decreasing behavior,  $V(\mathbf{q}_{\mu-1}) < V(\mathbf{q}_\mu) < V(\mathbf{q}_{\mu+1})$  or  $V(\mathbf{q}_{\nu-1}) > V(\mathbf{q}_\nu) > V(\mathbf{q}_{\nu+1})$ , which avoids that the curve be a non single-valued. Second, the consecutive points of the curve should be well separated which implies that,  $\Delta\mathbf{q}_\mu^T \Delta\mathbf{q}_\mu \geq \varepsilon_3 > 0$ , and ensures that the tangent vector is well defined. The threshold,  $\varepsilon_3$ , is taken as equal to the quotient between the length of the current polygonal curve  $C$  and the number of vertices. The algorithm assumes that the initial guess curve is an admissible “comparison curve”. Finally we say that the set of Hessian matrices used in step 3,  $\{\mathbf{H}_\mu\}_{\mu=1}^{\text{number of vertices}}$ , are updated rather than evaluated by using the procedure given in reference [16]. The above outlined algorithm is close in its basic philosophy to that proposed by Ayala and Schlegel [42].

The behavior of the above algorithm is shown for the location of the IRC curve on the Müller-Brown PES [44], joining the two minima labeled as, M1 and M2, with coordinates,  $x = -0.558$  length arbitrary units (*lau*),  $y = 1.442$  *lau* and  $x = -0.050$  *lau*,  $y = 0.467$  *lau*, respectively. A point of this IRC path is the FOSEP labeled as TS1 with coordinates,  $x = -0.822$  *lau*,  $y = 0.624$  *lau*. In figure 2 we show the initial guess curve  $C$ , which is a straight line ending in the points M1 and M2. The straight line is defined by a polygonal curve with ten vertices. These vertices will move during the location process according to the above algorithm, but the two ending points, M1 and M2, will remain fixed.

[Please insert figure 2 near here]

Figure 2 shows the  $\mathbf{e}_\mu$  vectors associated to each vertex of the polygonal curve  $C$ , computed according to the equation (23.b). The  $\mathbf{e}_\mu$  vector of a vertex is the gradient vector of the Weierstrass  $E$ -function with respect to the point location of the vertex,  $\mathbf{q}_\mu$ . These vectors are almost orthogonal to the tangent vectors of the straight line, except than that correspond to the vertices near to the ridge. In this case the two  $\mathbf{e}_\mu$  vectors are quasi orthogonal to the SD curve that follows the ridge.

[Please insert figure 3 near here]

1  
2  
3  
4  
5 As explained in the description of the algorithm, using the  $\mathbf{e}_\mu$  vectors and equation  
6 (23.c) we obtain the new coordinates of each vertex. This new set of coordinates and  
7 the associated  $\mathbf{e}_\mu$  are indicated in figure 3. However, the resulting polygonal curve  
8 defined by this new set of coordinates do not satisfy the requirements of regular curve  
9 to be a “comparison curve”, since the vertices 6 and 7 have the same value of the  
10 PES, they do not represent a real decrease of the PES as one moves on the curve from  
11 the ridge to the minimum M2. The vertex numbering starts at the first vertex located  
12 near the minimum M1. Due to this fact the parameterization of the new curve is  
13 needed. In this situation the parameterization consists in the displacement of the  
14 vertex 6 in the middle of the positions of the vertices 5 and 7. The resulting set of  
15 coordinates defines the new curve, not shown in the figure. With this new curve a  
16 new iteration begins.  
17  
18  
19  
20  
21  
22  
23  
24  
25  
26  
27

28 [Please insert figure 4 near here]  
29  
30  
31

32 In the middle of the localization process, the current curve  $C$  approach to the IRC  
33 curve. As shown in figure 4, vertices 8, 9, 10, which are near to the minimum M2, are  
34 located in the IRC curve. The corresponding  $\mathbf{e}_\mu$  vector of these vertices is a null  
35 vector. Finally in figure 5 we show the ten vertices located on the IRC curve, which  
36 means that the process is converged. Each  $\mathbf{e}_\mu$  vector is almost a null vector.  
37  
38  
39  
40  
41  
42

43 [Please insert figure 5 near here]  
44  
45  
46  
47  
48  
49

### 50 **3. THE THEORY OF DISCONTINUOUS EXTREMALS USED AS** 51 **ANALYSIS AND TREATMENT OF THE INTRINSIC REACTION** 52 **COORDINATE PATH PASSING THROUGH A VALLEY-RIDGE-** 53 **INFLECTION POINT** 54 55 56 57

58 As explained in sections 1 and 2, the IRC path at each point transverses orthogonally  
59 the set of equipotential curve levels, however in some cases an equipotential curve  
60

possesses null curvature at the point where the IRC cuts it and this point is the VRI point [12]. In this section we analyze the IRC path that from a FOSP deeps to other FOSP passing through a VRI point using the theory of discontinuous extremals. The theory of discontinuous extremals is an important subject of the full mathematical theory of CV. Notice that we are concerned with the type of VRI points where the gradient vector of this point is orthogonal to the eigenvector of zero eigenvalue of the Hessian matrix evaluated in this VRI point.

In the theory of CV, by a discontinuous extremal is meant an extremal curve having one or more corners. In such corners the tangent of the extremal curve has the ordinary discontinuities. The first additional necessary condition on extremal curve with corners is the Weierstrass-Erdmann corner condition, which says that, for homogeneous functional like that given in equation (2),  $\nabla_{d\mathbf{q}/dt} L(\mathbf{q}, d\mathbf{q}/dt)$ , must be continuous along the whole extremal curve. At each corner the above condition takes the form

$$\left[ \nabla_{d\mathbf{q}/dt} L(\mathbf{q}, d\mathbf{q}/dt) \right]_{d\mathbf{q}/dt=d\mathbf{q}^+/dt} - \left[ \nabla_{d\mathbf{q}/dt} L(\mathbf{q}, d\mathbf{q}/dt) \right]_{d\mathbf{q}/dt=d\mathbf{q}^-/dt} = \mathbf{0} \quad (24)$$

where  $d\mathbf{q}^-/dt$  and  $d\mathbf{q}^+/dt$  denote the tangent vectors of the extremal curve preceding and following the corner, respectively [40, 41]. Substituting equation (5) in equation (24) we obtain the Weierstrass-Erdmann corner condition for a discontinuous SD curve

$$v(\mathbf{q}) \frac{d\mathbf{q}^+/dt}{\sqrt{(d\mathbf{q}^+/dt)^T (d\mathbf{q}^+/dt)}} - v(\mathbf{q}) \frac{d\mathbf{q}^-/dt}{\sqrt{(d\mathbf{q}^-/dt)^T (d\mathbf{q}^-/dt)}} = \mathbf{0} \quad (25)$$

Since for the discontinuous SD curve, the tangent vectors preceding and following the corner are,  $d\mathbf{q}^-/dt = d\mathbf{q}/dt = \mathbf{g}$ , and  $d\mathbf{q}^+/dt = \mathbf{g}^+$ , respectively, then equation (25) is satisfied only at the stationary points of the PES, where  $v(\mathbf{q}) = [(\mathbf{g}(\mathbf{q}))^T \mathbf{g}(\mathbf{q})]^{1/2} = 0$ . The vectors,  $\mathbf{g}$  and  $\mathbf{g}^+$  are not collinear. In other words, the Weierstrass-Erdmann corner condition tells us the very well know fact that the SD curves branch only at the stationary points of the PES. The IRC curve is a SD curve such that emerging from the point  $\mathbf{q}_R = \mathbf{q}(t_0)$ , a stationary point of the PES character minimum, arrives at a FOSP of this PES and close to this point the tangent vector of this SD curve can be expressed as,  $\mathbf{g} = c \mathbf{v}_{TS}$ , being  $\mathbf{v}_{TS}$  the normalized eigenvector with negative eigenvalue of the Hessian matrix evaluated at the FOSP [27]. From all SD curves emerging from the  $\mathbf{q}_R$  point, one and only one of these curves, the IRC curve, arrives at a FOSP with normalized tangent,  $\mathbf{v}_{TS}$ . Since the FOSP is a stationary point of the



1  
 2  
 3  
 4  
 5  
 6  
 7  
 8  
 9  
 10  
 11  
 12  
 13  
 14  
 15  
 16  
 17  
 18  
 19  
 20  
 21  
 22  
 23  
 24  
 25  
 26  
 27  
 28  
 29  
 30  
 31  
 32  
 33  
 34  
 35  
 36  
 37  
 38  
 39  
 40  
 41  
 42  
 43  
 44  
 45  
 46  
 47  
 48  
 49  
 50  
 51  
 52  
 53  
 54  
 55  
 56  
 57  
 58  
 59  
 60

PES, then for the IRC curve this point is a corner point if we take, following this point, other SD curve with tangent vector orthogonal to the  $\mathbf{v}_{TS}$  vector. Notice that this corner point is an isolated point and does not belong to any curve such that each point of this curve is a corner point of each extremal curve of the field of extremals. In this way we have constructed a discontinuous SD curve such that starting at the  $\mathbf{q}_R$  point, the corner point is a FOSP of the PES. After following the corner, corresponding to the first FOSP, we take the SD curve that arrives at a next stationary point with character FOSP and, as before, close to this point its tangent vector is proportional to  $\mathbf{v}'_{TS}$  vector, being  $\mathbf{v}'_{TS}$  the normalized eigenvector with negative eigenvalue of the Hessian matrix corresponding to this second FOSP. The resulting discontinuous SD curve, the sub arc connecting the two FOSPs after following the first FOSP, should transverse a set of equipotential curve lines with negative curvature, since the tangent of this sub arc when it emerges from this stationary point is,  $d\mathbf{q}^+ / dt = \mathbf{g}^+$ , which is orthogonal to  $\mathbf{v}_{TS}$ . On the other hand walking to the second FOSP, the SD curve transverses a set of equipotential curve lines with positive curvature. As a consequence in this sub arc and due to the continuity property of the PES, the SD curve transverses at least an equipotential curve line with zero curvature, and the intersection point between this equipotential line and the SD curve is a VRI point. In this way we have constructed a discontinuous IRC curve, a discontinuous extremal curve, which passes through a VRI point and the corner is a FOSP. Now, we have the following question, does the above IRC discontinuous curve, which starts at the  $\mathbf{q}_R = \mathbf{q}(t_0)$  point and ends in the  $\mathbf{q}_P = \mathbf{q}(t_f)$  point, a stationary point of the PES character minimum associated to the products, minimizes the functional integral given in expression (2)? Before answering this question we study the behavior of the Weierstrass  $E$ -function for a SD curve around a corner point, a stationary point of the PES [45]. Taking equation (14) and the homogeneity condition of  $L(\mathbf{q}, d\mathbf{q}_C / dt)$  with respect to the argument  $d\mathbf{q}_C / dt$ , replacing  $d\mathbf{q}_C / dt$  by  $d\mathbf{q}^+ / dt = \mathbf{g}^+$ , and  $d\mathbf{q} / dt$  by  $d\mathbf{q}^- / dt = \mathbf{g}$ , the tangent vectors of the SD extremal curve preceding and following the corner respectively, and finally using equation (24), we obtain

$$\begin{aligned}
 & \left. (d\mathbf{q}^+ / dt)^T \left\{ \left[ \nabla_{d\mathbf{q}/dt} L(\mathbf{q}, d\mathbf{q}/dt) \right]_{d\mathbf{q}/dt=d\mathbf{q}^+/dt} - \left[ \nabla_{d\mathbf{q}/dt} L(\mathbf{q}, d\mathbf{q}/dt) \right]_{d\mathbf{q}/dt=d\mathbf{q}^-/dt} \right\} \right\} (26) \\
 & = E(\mathbf{q}, d\mathbf{q}^- / dt, d\mathbf{q}^+ / dt) = E(\mathbf{q}, \mathbf{g}, d\mathbf{q}^+ / dt) = E(\mathbf{q}, \mathbf{g}, \mathbf{g}^+) = 0
 \end{aligned}$$

According to the expression (26), the Weierstrass  $E$ -function of a discontinuous SD curve is zero at the corner. At this point it is interesting to study the variation of the



Weierstrass  $E$ -function preceding and following the corner. By differentiation equation (26) with respect to the parameter  $t$ , we find,

$$\begin{aligned} \frac{dE(\mathbf{q}, d\mathbf{q}^-/dt, d\mathbf{q}^+/dt)}{dt} &= (d\mathbf{q}^-/dt)^T [\nabla_{\mathbf{q}} L(\mathbf{q}, d\mathbf{q}^+/dt)] - (d\mathbf{q}^+/dt)^T [\nabla_{\mathbf{q}} L(\mathbf{q}, d\mathbf{q}^-/dt)] \\ &= -\frac{dE(\mathbf{q}, d\mathbf{q}^+/dt, d\mathbf{q}^-/dt)}{dt} \end{aligned} \quad (27)$$

Substituting as before,  $d\mathbf{q}^-/dt = \mathbf{g}$  and  $d\mathbf{q}^+/dt = \mathbf{g}^+$ , in equation (27), we find that for the SD curve, at the corner point,  $dE(\mathbf{q}, \mathbf{g}, \mathbf{g}^+)/dt = -dE(\mathbf{q}, \mathbf{g}^+, \mathbf{g})/dt = 0$ . In other words, preceding and following the corner of a SD curve, the two Weierstrass  $E$ -functions,  $E(\mathbf{q}, \mathbf{g}, \mathbf{g}^+)$ , and  $E(\mathbf{q}, \mathbf{g}^+, \mathbf{g})$ , the first decreases and the second increases, taking the value zero at the corner. Since for any SD curve the Weierstrass  $E$ -function is positive definite,  $E(\mathbf{q}, \mathbf{g}, d\mathbf{q}_C/dt) \geq 0$ , this conclusion is also extensible to discontinuous SD curves, since at the corner points the corresponding Weierstrass  $E$ -function takes the value zero. As mentioned in the previous section, the Weierstrass  $E$ -function gives the sufficient condition for an extremal curve to be a strong relative minimum for the functional integral like given in equation (2). However, applying this condition one assumes that the extremal discontinuous curve can be imbedded in a field of extremals, in this case a field of SD curves. In order to ensure that this is so, we make the following reasoning, the IRC is the only SD curve from all the set of curves starting at the  $\mathbf{q}_R = \mathbf{q}(t_0)$  point that it achieves the FOSP, playing the role of a corner point which does not belong to any corner curve. A corner curve is defined by the set of corner points of the field of discontinuous extremal curves. In other words no conjugate point exists with respect to the  $\mathbf{q}_R$  point when the IRC curve arrives to the corner point. From the corner point, the first FOSP, to the second FOSP only a SD curve exists connecting both FOSPs and the minimum  $\mathbf{q}_P = \mathbf{q}(t_f)$ . Taking into account all the domain of the discontinuous IRC curve,  $t_0 \leq t \leq t_f$ , we conclude that in this domain the discontinuous curve does not possess any conjugate point with respect to the  $\mathbf{q}_R$  point and due to this fact the discontinuous IRC curve with endpoints,  $\mathbf{q}_R = \mathbf{q}(t_0)$  and  $\mathbf{q}_P = \mathbf{q}(t_f)$ , can be imbedded in the field of SD curves with starting point,  $\mathbf{q}_R = \mathbf{q}(t_0)$ , a stationary point of the PES character minimum. From the above results, we conclude that the discontinuous IRC curve, constructed as explained above, is an extremal curve strong relative minimum.

1  
 2  
 3  
 4  
 5  
 6  
 7  
 8  
 9  
 10  
 11  
 12  
 13  
 14  
 15  
 16  
 17  
 18  
 19  
 20  
 21  
 22  
 23  
 24  
 25  
 26  
 27  
 28  
 29  
 30  
 31  
 32  
 33  
 34  
 35  
 36  
 37  
 38  
 39  
 40  
 41  
 42  
 43  
 44  
 45  
 46  
 47  
 48  
 49  
 50  
 51  
 52  
 53  
 54  
 55  
 56  
 57  
 58  
 59  
 60

We conclude this section by analyzing, from the point of view of the above exposed theory of the second variation, the treatment used some times consisting in deviating the IRC curve from the original valley floor to other valley floor or approximation to it rather than following the ridge when the path finds a VRI point. The question is, which is the error produced when one takes this deviation on the light of the above analysis? For this purpose let us denote the VRI point by  $\mathbf{q}_{VRI} = \mathbf{q}(t_{VRI})$ . From the point  $\mathbf{q}_R = \mathbf{q}(t_0)$ , a stationary point of the PES character minimum, we construct a central field of SD curves. In this region covered by this field the integral,  $J_R(\mathbf{q}) = \Delta V_{R \rightarrow \mathbf{q}}(\mathbf{q}) = V(\mathbf{q}) - V(\mathbf{q}_R)$ , is defined, which again is the value of the first two integrals of equation (4) evaluated along any curve defined in this region joining the point  $\mathbf{q}_R$  to the variable point  $\mathbf{q}$ . One of the SD curves of this field connects the  $\mathbf{q}_R$  point with the FO SP which is taken as a corner and from this corner it leads to the next FO SP passing through the VRI point,  $\mathbf{q}_{VRI}$ . The just defined SD curve or extremal curve is the discontinuous IRC curve. Now let  $V_{VRI}$  the equipotential curve of the family of curves,  $J_R(\mathbf{q}) = \text{constant}$ , such that the discontinuous IRC intersects with this curve at the point  $\mathbf{q}_{VRI}$ . This equipotential curve,  $V_{VRI}$ , also intersects at the point  $\mathbf{q}_M$  with the SD curve that emerges from the point  $\mathbf{q}_R$  and follows a valley floor or near to it. Finally, let  $C$  a curve obtained from the discontinuous IRC curve by replacing the sub arc of this discontinuous IRC from  $\mathbf{q}_R$  to  $\mathbf{q}_{VRI}$  by the curve joining the points  $\mathbf{q}_R$ ,  $\mathbf{q}_M = \mathbf{q}(t_M)$ , and  $\mathbf{q}_{VRI}$ , where the sub arc of the curve  $C$  connecting the points  $\mathbf{q}_R$ , and  $\mathbf{q}_M$ , is the SD curve that is located in a valley floor or near to it, while the curve connecting the points  $\mathbf{q}_M$ , and  $\mathbf{q}_{VRI}$ , is a sub arc of the equipotential curve  $V_{VRI}$ . We denote by  $d\mathbf{q}_C / dt$  the tangent vector of this arbitrary curve  $C$ . According to this construction, the sub arc of the curve  $C$  located between the points,  $\mathbf{q}_M = \mathbf{q}(t_M)$  and  $\mathbf{q}_{VRI}$ , the tangent vector of this  $C$  curve,  $d\mathbf{q}_C / dt$ , is the tangent of the equipotential curve  $V_{VRI}$ , which implies that this tangent vector at each point is orthogonal to the gradient vector  $\mathbf{g}(\mathbf{q})$  at this point in this sub arc. Notice that between these points,  $\mathbf{q}_M$  and  $\mathbf{q}_{VRI}$ , and according to equation (17), the Weierstrass  $E$ -function for the  $C$  curve at each point is equal to  $L(\mathbf{q}, d\mathbf{q}_C/dt)$ . With all this set of definitions and considerations, it is easy to see that the line integral of the Weierstrass  $E$ -function for this curve  $C$  is,

$$\begin{aligned}
\int_{t_0}^{t_f} E(\mathbf{q}, \mathbf{g}, d\mathbf{q}_C/dt') dt' &= \frac{1}{2} \int_{t_0}^{t_f} \left( 2 - \frac{2\mathbf{g}^T (d\mathbf{q}_C/dt')}{\sqrt{\mathbf{g}^T \mathbf{g}} \sqrt{(d\mathbf{q}_C/dt')^T (d\mathbf{q}_C/dt')}} \right) L(\mathbf{q}, d\mathbf{q}_C/dt') dt' \\
&= \int_{t_0}^{t_M} E(\mathbf{q}, \mathbf{g}, d\mathbf{q}_C/dt') dt' + \int_{t_M}^{t_{VRI}} E(\mathbf{q}, \mathbf{g}, d\mathbf{q}_C/dt') dt' + \int_{t_{VRI}}^{t_f} E(\mathbf{q}, \mathbf{g}, d\mathbf{q}_C/dt') dt' \\
&= \int_{t_M}^{t_{VRI}} L(\mathbf{q}, d\mathbf{q}_C/dt') dt' > 0
\end{aligned} \tag{28}$$

where equation (22) has been used. The integrals evaluated in the intervals,  $[t_0, t_M]$  and  $[t_{VRI}, t_f]$ , are zero because these two integrals are computed on a SD curve,  $d\mathbf{q}_C/dt = \mathbf{g}(\mathbf{q})$ . In more detail, the  $C$  curve coincides with the SD sub arc that contains the points,  $\mathbf{q}_{VRI} = \mathbf{q}(t_{VRI})$  and  $\mathbf{q}_P = \mathbf{q}(t_f)$ , a sub arc of the discontinuous IRC connecting the points,  $\mathbf{q}_R = \mathbf{q}(t_0)$  and  $\mathbf{q}_P = \mathbf{q}(t_f)$ . Finally, between the points,  $\mathbf{q}_R = \mathbf{q}(t_0)$  and  $\mathbf{q}_M = \mathbf{q}(t_M)$ , the  $C$  curve coincides, by construction, with a sub arc of the SD curve that emerges from the point,  $\mathbf{q}_R$ , follows a valley floor or near to it and passes through the point  $\mathbf{q}_M$ .

This result shows that the discontinuous IRC curve connecting the points,  $\mathbf{q}_R = \mathbf{q}(t_0)$  and  $\mathbf{q}_P = \mathbf{q}(t_f)$ , which in some region of its domain passes through a ridge, minimizes the integral (2) with respect to any other curve imbedded in this field of the SD curves even if this arbitrary curve in all its domain passes through a valley ridge or near to it. As pointed out many times by Quapp and coworkers [46, 47], starting at the FO SP, where  $N - 1$  eigenvalues of the eigenvectors orthogonal to the decay eigenvector are positive definite, the IRC has the MEP property or in others words is the true RP. Nevertheless, the IRC can lose this property but even in this situation the IRC minimizes integral (2) evaluated between the points  $\mathbf{q}_R$  and  $\mathbf{q}_P$ . We conclude this section by analyzing, from the point of view of the above exposed theory of the second variation applied to discontinuous extremals, the treatment used some times consisting in deviating the IRC curve from the original valley floor to other valley floor or approximation to it rather than following the ridge when the IRC path finds a VRI point. In order to be clear with respect to the above concepts, we refer to figure 6 where a two dimensional representation of the key elements of the following discussion is exemplified on the PES used by Quapp in his studies about the VRI problem [46].

[Please insert figure 6 near here]

In this example the discontinuous IRC, described by the thin dashed line, can start either in the minimum situated in the top left or one of the minima located in the bottom. We start the description of the discontinuous IRC in the minimum located in the left bottom with coordinates,  $x = -1.144 \text{ lau}$ ,  $y = -3.070 \text{ lau}$ , labeled as  $\mathbf{q}_R$  and outside of the figure. The minimum located at the top left is labeled as  $\mathbf{q}_P$  and is also located outside the figure. The coordinates of the  $\mathbf{q}_P$  point are,  $x = -11.190 \text{ lau}$ ,  $y = 11.190 \text{ lau}$ . Starting at  $\mathbf{q}_R$  point the IRC curve finds the FOSP, labeled as FOSP1, located at  $x = 0.789 \text{ lau}$ ,  $y = -0.789 \text{ lau}$ . This FOSP1 point is also the corner point of the discontinuous IRC, since after this point the IRC path takes a new direction which is parallel to the eigenvector of the Hessian matrix at this FOSP1 point orthogonal to the eigenvector with negative eigenvalue, in other words,  $d\mathbf{q}^+ / dt |_{FOSP1} = c \mathbf{v}$ , where  $\mathbf{v}$  is the eigenvector with positive eigenvalue. When the discontinuous IRC curve leads from the FOSP1 it finds a VRI point,  $\mathbf{q}_{VRI}$ , located at  $x = 0.0 \text{ lau}$ ,  $y = 0.0 \text{ lau}$ , [46], and finally it arrives at the second FOSP, labelled as FOSP2. The FOSP2 point is located at the point with coordinates,  $x = -0.849 \text{ lau}$ ,  $y = 0.849 \text{ lau}$ . Finally the discontinuous IRC curve deeps from the FOSP2 to the  $\mathbf{q}_P$  point. On the other hand the curve  $C$ , emerges from the  $\mathbf{q}_R$  point and it follows initially a SD curve near the IRC path that emerges also from the same point and arrives at the FOSP1. This SD curve, near the FOSP1 and before arriving to it, changes the direction in a continuous way and leads to the point labelled as M,  $\mathbf{q}_M$ , located in the equipotencial curve line that contains the VRI point. The coordinates of the M point are,  $x = -0.09 \text{ lau}$ ,  $y = -0.09 \text{ lau}$ . The M point is very close to the VRI point. Notice that the sub arc of the equipotencial curve line defined between the points M and VRI is also a sub arc of the curve  $C$ . Finally, from the VRI point the curve  $C$  leads to the FOSP2 and falls into the  $\mathbf{q}_P$  minimum following the same path of the discontinuous IRC curve. Now, taking the distance between the points M and VRI and the norm of the gradient vector at the M point,  $\mathbf{g}(\mathbf{q}_M)$ , we evaluate in an approximate manner the last integral of equation (28). In other words, since the  $\mathbf{q}_M$  point is very close to the  $\mathbf{q}_{VRI}$  point, then the calculation proceeds as follows,

$$\begin{aligned}
& \int_{t_0}^{t_{VRI}} E(\mathbf{q}_C, \mathbf{g}, d\mathbf{q}_C/dt') dt' = \int_{t_M}^{t_{VRI}} L(\mathbf{q}_C, d\mathbf{q}_C/dt') dt' \approx \sum_{\mu=M}^{VRI-1} [\mathbf{g}_\mu^T \mathbf{g}_\mu]^{1/2} [\Delta \mathbf{q}_\mu^T \Delta \mathbf{q}_\mu]^{1/2} \\
& \approx [\mathbf{g}_M^T \mathbf{g}_M]^{1/2} [\Delta \mathbf{q}_M^T \Delta \mathbf{q}_M]^{1/2} = [\mathbf{g}_M^T \mathbf{g}_M]^{1/2} [(\mathbf{q}_{VRI} - \mathbf{q}_M)^T (\mathbf{q}_{VRI} - \mathbf{q}_M)]^{1/2} \quad (29) \\
& = 1.420 \cdot 0.090 = 0.128 \text{ eau}
\end{aligned}$$

where,  $\mathbf{g}_\mu = \mathbf{g}(\mathbf{q}_\mu)$ ,  $\Delta \mathbf{q}_\mu = \mathbf{q}_{\mu+1} - \mathbf{q}_\mu$ , and eau means energy arbitrary units. This is the error committed when the curve  $C$  asides the VRI point to avoid following the SD curve locate in the ridge, which is the sub arc of the correct the discontinuous IRC path joining the pints  $\mathbf{q}_R$  and  $\mathbf{q}_P$ .

#### 4. CONCLUSIONS

The mathematical techniques used in the integration of both total and partial differential equations that appear in the theory of CV provide the bases of the proposed algorithms of the integration of the IRC equation (1). The reason is due to the fact that the IRC path is an extremal curve of a variational problem of the functional type,  $L(\mathbf{q}, d\mathbf{q}/dt)$ , where this functional is homogeneous of degree one with respect to the tangent vector,  $d\mathbf{q}/dt$ .

The set of recently proposed algorithms to locate the IRC curve in the PES based on the minimization of the normal force to the curve can be seen as computational techniques consisting in the minimization, until zero value, of the line integral of the Weierstrass  $E$ -function. The Weierstrass  $E$ -function represents one of the most important elements of the set of necessary and sufficient conditions to guarantee that an extremal curve minimizes (maximizes) a functional integral like that given in equation (2). On the other hand, we have proposed an algorithm based on the direct minimization of the line integral of the Weierstrass  $E$ -function to locate the IRC curve. In addition each step of this algorithm is justified according to the theory of CV.

Finally, the theory of broken extremal curves has been used to analyze the IRC path when a point of this path is a VRI point. The above results clearly show from the theory of CV that the IRC curve model can lose the RP character but even in this situation and compared with an arbitrary curve constructed in the way that preserves the RP character, is the best curve in the sense that it minimizes the integral (2). From

the theory of CV, to look for the curve that satisfies the RP requirements will consist in finding the adequate functional of the type,  $L(\mathbf{q}, d\mathbf{q}/dt)$ , such that in the resulting extremal curve each point of this curve is located in a valley floor of the PES connecting two minima through a FOSEP.

## APPENDIX A: INTEGRATION OF THE PARTIAL DIFFERENTIAL EQUATION (6)

We take as a solution of the partial differential equation (6) of the form

$$U(\mathbf{q}, \mathbf{q}_R) = J_R(\mathbf{q}) + f(\mathbf{q}_R) = \mathbf{g}_R^T (\mathbf{q} - \mathbf{q}_R) + 1/2 (\mathbf{q} - \mathbf{q}_R)^T \mathbf{H}_R (\mathbf{q} - \mathbf{q}_R) + f(\mathbf{q}_R) \quad (\text{A.1})$$

where,  $\mathbf{g}_R = \mathbf{g}(\mathbf{q}_R)$ ,  $\mathbf{H}_R = \mathbf{H}(\mathbf{q}_R)$ , being  $\mathbf{H}(\mathbf{q}) = \nabla_{\mathbf{q}} \nabla_{\mathbf{q}}^T V(\mathbf{q})$ . We assume that  $\mathbf{H}_R$  is independent of  $\mathbf{q}$ , and,  $\det \mathbf{H}_R \neq 0$ , in a domain around  $\mathbf{q}_R$ , without loss of generality. If  $J_R(\mathbf{q})$  is a solution of the Hamilton-Jacobi equation (6), depending on  $N$  parameters,  $\mathbf{q}_R$ , then  $U(\mathbf{q}, \mathbf{q}_R)$  is also a solution labeled complete integral, which depends on  $N + 1$  parameters, namely, the vector  $\mathbf{q}_R$  and the scalar  $f(\mathbf{q}_R)$ . Notice that the  $N + 1$ -th parameter,  $f(\mathbf{q}_R)$ , is additive since only derivatives of  $J_R$  with respect to  $\mathbf{q}$  vector appears in equation (6). The determinant condition,  $\det (\nabla_{\mathbf{q}} \nabla_{\mathbf{q}_R}^T U(\mathbf{q}, \mathbf{q}_R)) = \det \mathbf{H}_R \neq 0$ , is satisfied in the domain of the  $\mathbf{q}$ ,  $J_R$ -space under consideration. According to the discussion of subsection 2.A, the envelope of an arbitrary  $N$ -parameter family of solutions is also a solution. The envelope is obtained from

$$\nabla_{\mathbf{q}_R} U(\mathbf{q}, \mathbf{q}_R) = \nabla_{\mathbf{q}_R} J_R(\mathbf{q}) + \nabla_{\mathbf{q}_R} f(\mathbf{q}_R) = -\mathbf{g}_R - \mathbf{H}_R (\mathbf{q} - \mathbf{q}_R) + \nabla_{\mathbf{q}_R} f(\mathbf{q}_R) = \mathbf{0} \quad (\text{A.2a})$$

and eliminating from the equations (A.1) and (A.2a) the vector parameter  $\mathbf{q}_R$ . Using the explanation given in subsection 2.A, for each  $\mathbf{q}_R$  parameter, the intersection of the resulting envelope with  $J_R(\mathbf{q})$  is a characteristic curve. The envelope corresponds to the integral surface introduced in subsection 2.A, and is traced out by allowing that  $\mathbf{q}_R$  takes any real value. We emphasize that the projection of the characteristic curve in the  $\mathbf{q}$  space, given by equation (A.2a), is the equation of the extremal curve, which in the present case is the SD curve. The function  $f(\mathbf{q}_R)$  is arbitrary, using this fact the vector,  $\nabla_{\mathbf{q}_R} f(\mathbf{q}_R) = \Delta \mathbf{g}_R + \mathbf{g}_R$ , can be chosen in an arbitrary manner, then using this



fact and that  $\det(\nabla_{\mathbf{q}}\nabla_{\mathbf{q}_R}^T U(\mathbf{q}, \mathbf{q}_R)) = \det \mathbf{H}_R \neq 0$ , from equation (A.2a) we obtain  $\mathbf{q}$  as a function of  $\mathbf{q}_R$  and  $\Delta\mathbf{g}_R$ . Now, from the equation

$$\nabla_{\mathbf{q}} U(\mathbf{q}, \mathbf{q}_R) = \nabla_{\mathbf{q}} J_R(\mathbf{q}) = \mathbf{g}_R + \mathbf{H}_R(\mathbf{q} - \mathbf{q}_R) = \mathbf{p} \quad (\text{A.2b})$$

and equation (A.2a), we obtain the  $\mathbf{p}$  vector as a function of  $\Delta\mathbf{g}_R$ .

In order to prove that the vector functions  $\mathbf{q}$  and  $\mathbf{p}$  determined in this way, satisfy the differential equations (12), we first differentiate the equation (A.2a) with respect to  $t$  and the equation (6) with respect to  $\mathbf{q}_R$ , after the substitution of  $J_R(\mathbf{q})$  as that given in equation (A.1). In this way we have the two equations,

$$\left[\nabla_{\mathbf{q}}\nabla_{\mathbf{q}_R}^T U(\mathbf{q}, \mathbf{q}_R)\right]\frac{d\mathbf{q}}{dt} = \left[\nabla_{\mathbf{q}}\nabla_{\mathbf{q}_R}^T J_R(\mathbf{q})\right]\frac{d\mathbf{q}}{dt} = \mathbf{H}_R\left(\frac{d\mathbf{q}}{dt}\right) = \mathbf{0} \quad (\text{A.3a})$$

$$\left[\nabla_{\mathbf{q}}\nabla_{\mathbf{q}_R}^T J_R(\mathbf{q})\right]\nabla_{\mathbf{p}} F(\mathbf{q}, \nabla_{\mathbf{q}} J_R(\mathbf{q})) = \mathbf{H}_R \nabla_{\mathbf{p}} F(\mathbf{q}, \nabla_{\mathbf{q}} J_R(\mathbf{q})) = \mathbf{H}_R \mathbf{p} = \mathbf{0} \quad (\text{A.3b})$$

Subtracting equation (A.3b) from equation (A.3a), we obtain equation (13.a), since  $\det(\mathbf{H}_R) \neq 0$ . Finally, substituting the  $\mathbf{p}$  vector as given in the equation (A.2b) we get

$$\frac{d\mathbf{q}}{dt} = \mathbf{p} = \mathbf{g}_R + \mathbf{H}_R(\mathbf{q} - \mathbf{q}_R) \quad (\text{A.4})$$

After integration of equation (A.4) we obtain

$$\mathbf{q}(t) = \mathbf{q}_R - \left[\mathbf{I} - \exp(\mathbf{H}_R(t - t_0))\right]\mathbf{H}_R^{-1}\mathbf{g}_R \quad (\text{A.5})$$

where  $\mathbf{I}$  is the unit matrix. Equation (A.5) is a very well known expression reported many times in the literature on the studies about the IRC path, e.g. see reference [27]. Now we differentiate equation (A.2b) with respect to  $t$  and equation (6) with respect to  $\mathbf{q}$  after being substituted  $J_R(\mathbf{q})$  function given in equation (A.1). With these operations we obtain,

$$\left[\nabla_{\mathbf{q}}\nabla_{\mathbf{q}}^T U(\mathbf{q}, \mathbf{q}_R)\right]\frac{d\mathbf{q}}{dt} = \left[\nabla_{\mathbf{q}}\nabla_{\mathbf{q}}^T J_R(\mathbf{q})\right]\frac{d\mathbf{q}}{dt} = \mathbf{H}_R\left(\frac{d\mathbf{q}}{dt}\right) = \frac{d\mathbf{p}}{dt} = \frac{d}{dt}\left[\nabla_{\mathbf{q}} J_R(\mathbf{q})\right] \quad (\text{A.6a})$$

$$\left[\nabla_{\mathbf{q}}\nabla_{\mathbf{q}}^T J_R(\mathbf{q})\right]\nabla_{\mathbf{p}} F(\mathbf{q}, \nabla_{\mathbf{q}} J_R(\mathbf{q})) + \nabla_{\mathbf{q}} F(\mathbf{q}, \nabla_{\mathbf{q}} J_R(\mathbf{q})) = \mathbf{H}_R \mathbf{p} - \frac{1}{2}\nabla_{\mathbf{q}} v^2(\mathbf{q}) = \mathbf{0} \quad (\text{A.6b})$$

Subtracting equation (A.6b) from equation (A.6a), and using equation (A.4) we get equation (13.c). However, in the present case the integrated form for  $\mathbf{p}$  can be obtained by substituting equation (A.5) in equation (A.2b), resulting the well know result,

$$\mathbf{p}(t) = \exp(\mathbf{H}_R(t - t_0))\mathbf{g}_R \quad (\text{A.7})$$

From equation (A.7) and equation (A.6b), where,  $1/2 \nabla_{\mathbf{q}} v^2(\mathbf{q}) = \mathbf{H}_R \mathbf{g}(\mathbf{q})$ , we observe that,  $\mathbf{p}(t) = \mathbf{g}(\mathbf{q}(t))$  and  $\mathbf{p}(t_0) = \mathbf{p}_R = \mathbf{g}_R = \mathbf{g}(\mathbf{q}(t_0))$ . Finally, substituting equation (A.5) in the  $J_R(\mathbf{q})$  expression given in equation (A.1) we get

$$J_R(\mathbf{q}(t)) = \frac{1}{2} \mathbf{g}_R^T \exp(\mathbf{H}_R(t-t_0)) \mathbf{H}_R^{-1} \exp(\mathbf{H}_R(t-t_0)) \mathbf{g}_R - \frac{1}{2} \mathbf{g}_R^T \mathbf{H}_R^{-1} \mathbf{g}_R \quad (\text{A.8})$$

Equation (A.8) is the integrated form of equation (13.b). We conclude this appendix saying that the above procedure is a trivial application of the Jacobi method to integrate non-linear first-order partial differential equations [15] like that given in equation (6).

## ACKNOWLEDGMENTS

Financial support from the Spanish *Ministerio de Ciencia y Tecnología*, DGI project CTQ2005-01117/BQU and, in part from the *Generalitat de Catalunya* projects 2005SGR-00111 and 2005SGR-00175 is fully acknowledged. Ramon Crehuet gratefully acknowledges the *Ramón y Cajal Program*. Antoni Aguilar-Mogas gratefully thanks to *Ministerio de Ciencia y Tecnología* for a predoctoral fellowship.



1  
2  
3  
4  
5  
6  
7  
8  
9  
10  
11  
12  
13  
14  
15  
16  
17  
18  
19  
20  
21  
22  
23  
24  
25  
26  
27  
28  
29  
30  
31  
32  
33  
34  
35  
36  
37  
38  
39  
40  
41  
42  
43  
44  
45  
46  
47  
48  
49  
50  
51  
52  
53  
54  
55  
56  
57  
58  
59  
60

### FIGURE CAPTIONS

Figure 1. At each variational problem like that given in equation (2) where the integrand,  $L(\mathbf{q}, d\mathbf{q} / dt)$ , is positive definite we can correspond to each line element,  $(\mathbf{q}, d\mathbf{q} / dt)$  a vector with the same direction and parallel to the vector  $d\mathbf{q} / dt$  with components  $\xi d\mathbf{q} / dt$  such that  $L(\mathbf{q}, \xi d\mathbf{q} / dt) = 1$ . To be consistent with the main text, the vector  $\xi d\mathbf{q} / dt$  will be denoted as  $d\mathbf{q} / dt$ . The equation,  $L(\mathbf{q}, d\mathbf{q} / dt) = 1$ , defines a surface in the space of the  $d\mathbf{q} / dt$  vectors, and depends parametrically of  $\mathbf{q}$  and is called the indicatrix of the variational problem under consideration at the point  $\mathbf{q}$ . The indicatrix surface is obtained as follows, on each path passing through the point  $\mathbf{q}$  we take a sub arc of this path such that the line integral given in equation (2) with  $L(\mathbf{q}, d\mathbf{q} / dt) = 1$  along this sub arc takes the value  $dV > 0$ . The value  $dV$  is the radius length of the indicatrix. The line integral evaluated on the sub arc of the SD curve passing through the point  $\mathbf{q}$ , takes the value,  $dJ = dV$ , since is a curve of this indicatrix with radius length  $dV$ . The line element of the extremal curve,  $(\mathbf{q}, d\mathbf{q}_{SD} / dt)$ , which corresponds to the point  $d\mathbf{q}_{SD} / dt$  of the indicatrix and the tangent plane touching the indicatrix at this point  $d\mathbf{q}_{SD} / dt$  must be tangent to the contour line of the PES,  $V = con_2$ . The arbitrary path,  $\mathbf{q}_C(t)$ , with line element  $(\mathbf{q}, d\mathbf{q}_C / dt)$  touches the indicatrix at the point  $d\mathbf{q}_C / dt$ . A perpendicular vector from the point  $d\mathbf{q}_C / dt$  to the above tangent plane is build touching it at the point  $d\mathbf{q}' / dt$ . By the construction, the resulting perpendicular vector,  $d\mathbf{q}' / dt - d\mathbf{q}_C / dt$ , is proportional to the vector,  $d\mathbf{q}_{SD} / dt$ , being this proportionality factor the Weierstrass  $E$ -function,  $E(\mathbf{q}, \mathbf{g}, d\mathbf{q}_C / dt)$ , where  $\mathbf{g} = d\mathbf{q}_{SD} / dt$ .

Figure 2. Equipotential curve lines of the Muller-Brown PES reported in reference [44]. The bold line is the guess polygonal curve  $C$ . Each cross indicates the point where the vertex is located. The arrows are the  $\mathbf{e}_\mu$  vectors evaluated according to the equation (23.b). Each  $\mathbf{e}_\mu$  vector is the gradient vector of the Weierstrass  $E$ -function with respect to the position of the vertex.

Figure 3. Equipotential curve lines of the Muller-Brown PES reported in reference [44]. The crosses represent the position of the vertices that define the polygonal  $C$  curve. The position of the vertices is obtained from line minimization, using equation

1  
2  
3  
4 (23.c), of the set of vertices described in figure 2. This new set of vertices does not  
5 describe a regular curve to be a “comparison curve”, which implies a new  
6 parameterization of the polygonal curve  $C$ . See text for more details.  
7  
8  
9

10  
11 Figure 4. Equipotential curve lines of the Muller-Brown PES reported in reference  
12 [44]. The crosses represent the position of the vertices that define the polygonal  $C$   
13 curve. The bold line is the polygonal curve  $C$ . Notice that this polygonal curve  
14 satisfies the requirements of “comparison curve”. At this step of the iterations  
15 process, some vertices are already locate on the IRC curve, the corresponding norm of  
16  $\mathbf{e}_\mu$  vector is below to a given threshold.  
17  
18  
19  
20  
21  
22

23  
24 Figure 5. Equipotential curve lines of the Muller-Brown PES reported in reference  
25 [44]. The crosses represent the position of the vertices. In this case each vertex is  
26 located on the IRC curve joining the minima M1 and M2. The bold line is the  
27 polygonal IRC curve.  
28  
29  
30  
31

32  
33 Figure 6. Equipotential curve lines of the PES reported in reference [46] for  $\mu = 2$ ,  
34 which corresponds to a valley-ridge symmetric problem. The thin dashed line draws  
35 the discontinuous IRC path joining the minima, P, situated at the top left (labeled as  
36  $\mathbf{q}_P$  in the main text) and R at the bottom left (labeled as  $\mathbf{q}_R$  in the main text) passing  
37 through the two first order saddle points labeled as FOSP1 and FOSP2. The  
38 stationary point, FOSP1, is the corner point of the discontinuous IRC path. The bold  
39 dashed line is the  $C$  curve. A sub arc of this  $C$  curve coincides with the IRC curve  
40 that joins the points R and VRI (labeled as  $\mathbf{q}_{VRI}$  in the main text). Other sub arc of this  
41  $C$  curve joins the points M (labeled as  $\mathbf{q}_M$  in the main text) and the minimum R and  
42 corresponds to a sub arc of a SD curve that emerges from the minimum R and is  
43 neighbor to the IRC path that goes from the first order saddle point, FOSP1, to the  
44 minimum R. Finally, the enlarged figure shows the sub arc of the curve  $C$  connecting  
45 the points M and VRI lying on the same equipotential curve. This sub arc is the  
46 domain of the curve  $C$  where the line integral of the Weierstrass  $E$ -function is  
47 different from zero and its integrand between M and VRI points coincides with the  
48 functional  $L(\mathbf{q}, d\mathbf{q}_C/dt)$ .  
49  
50  
51  
52  
53  
54  
55  
56  
57  
58  
59  
60

Figure 1

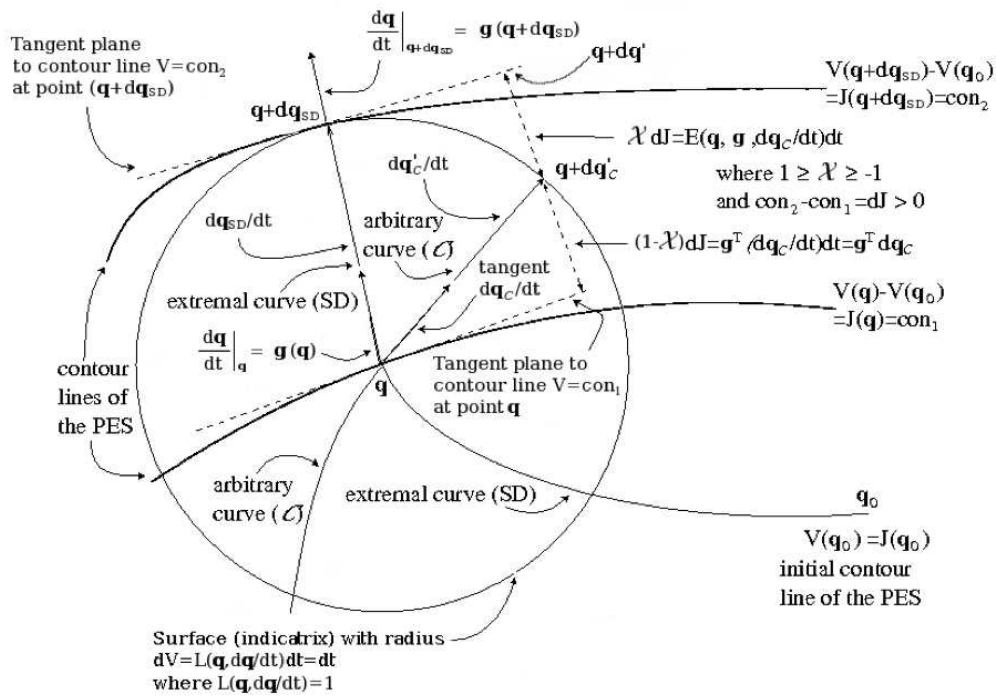
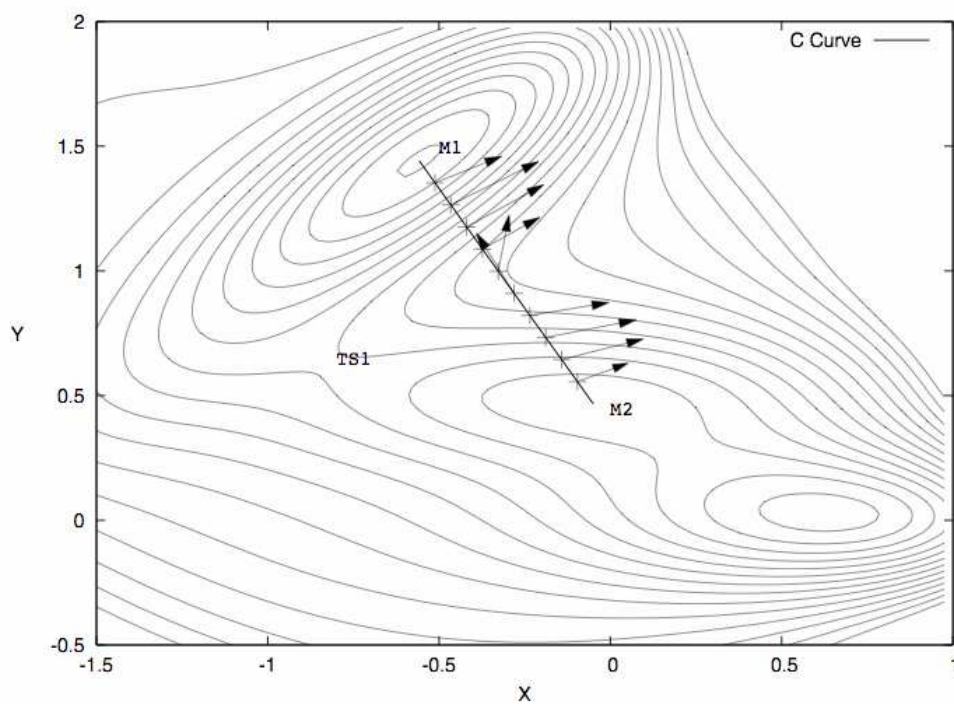
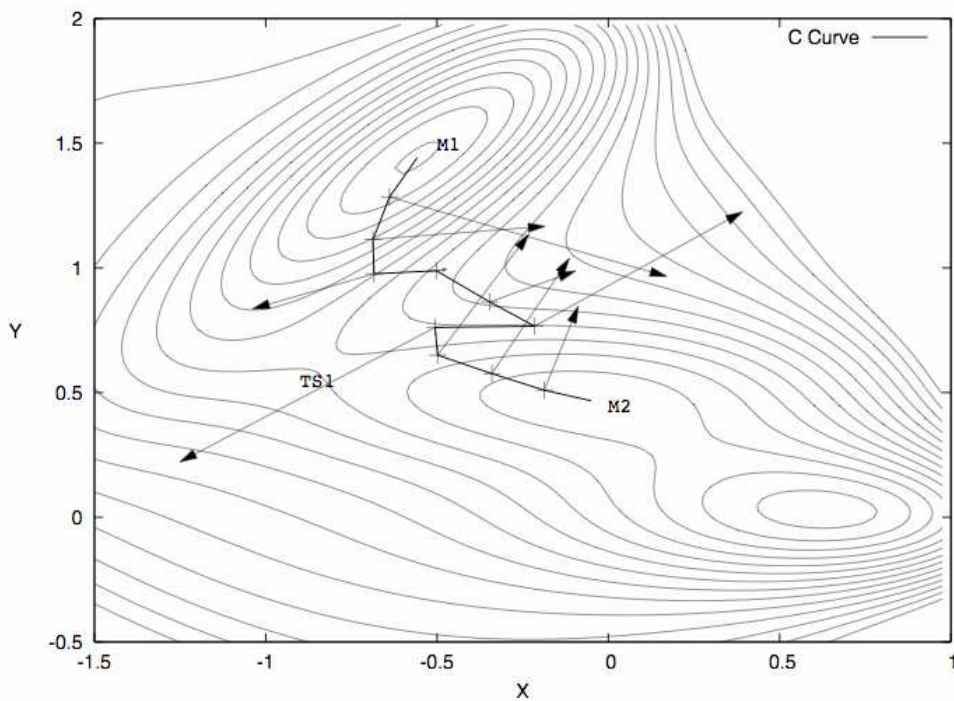


Figure 2



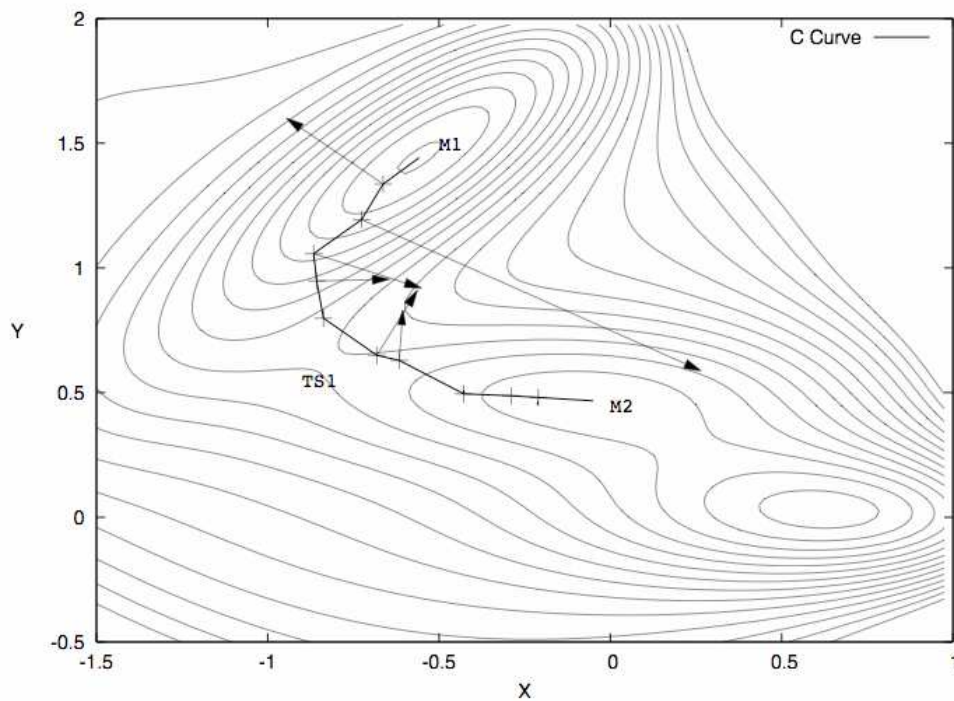
ew Only

Figure 3



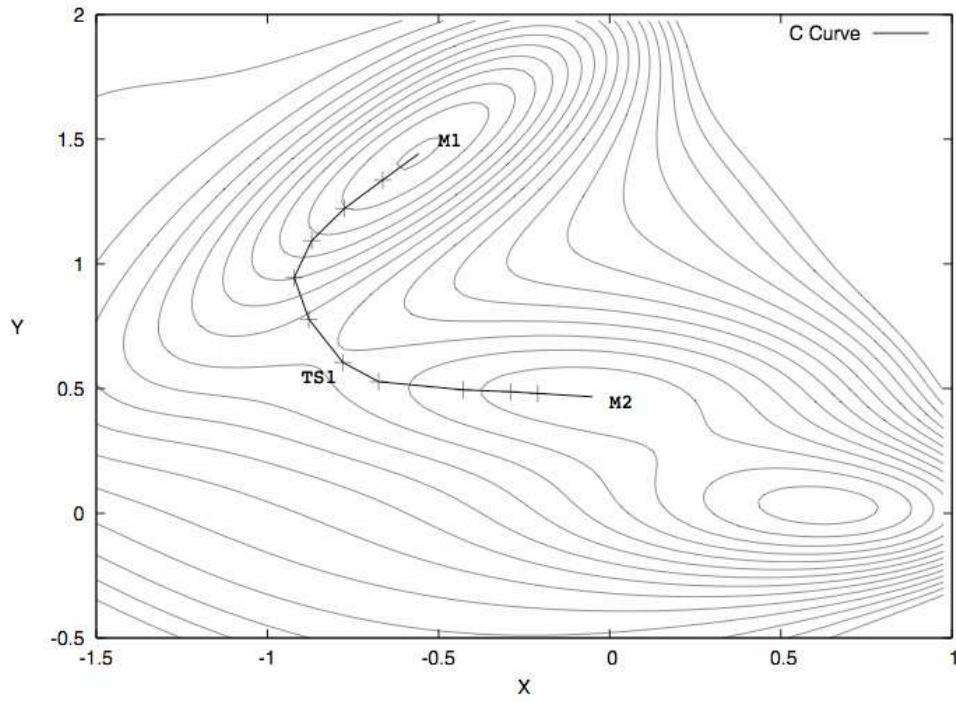
ew Only

Figure 4



ew Only

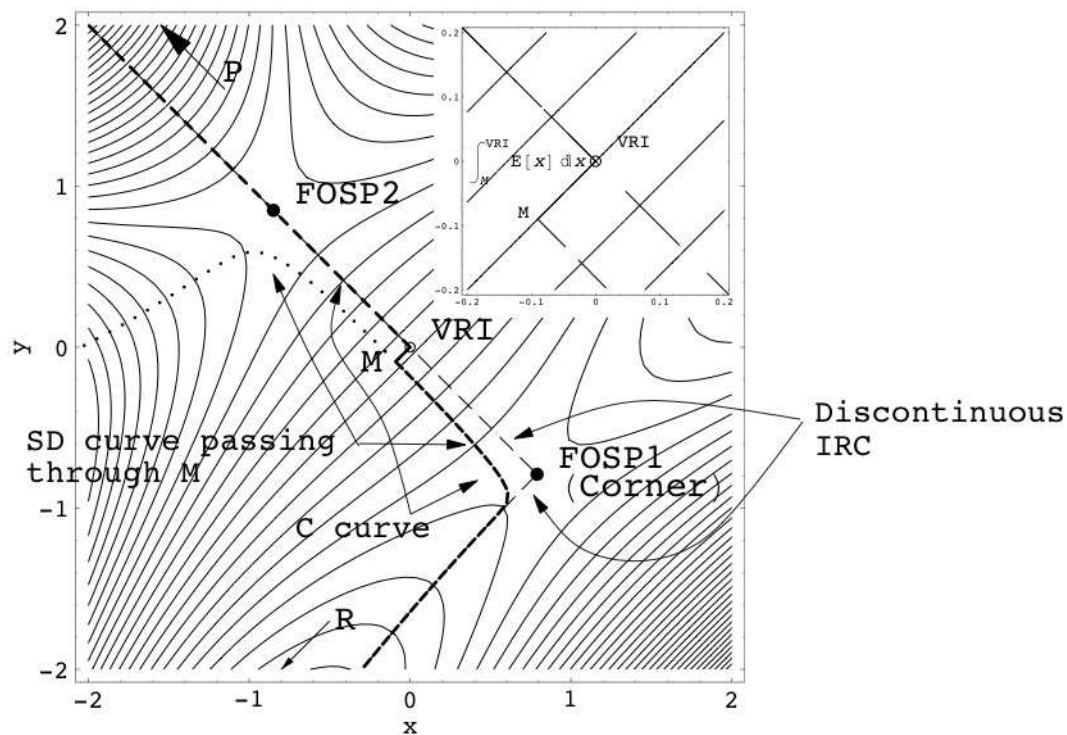
Figure 5



ew Only



Figure 6



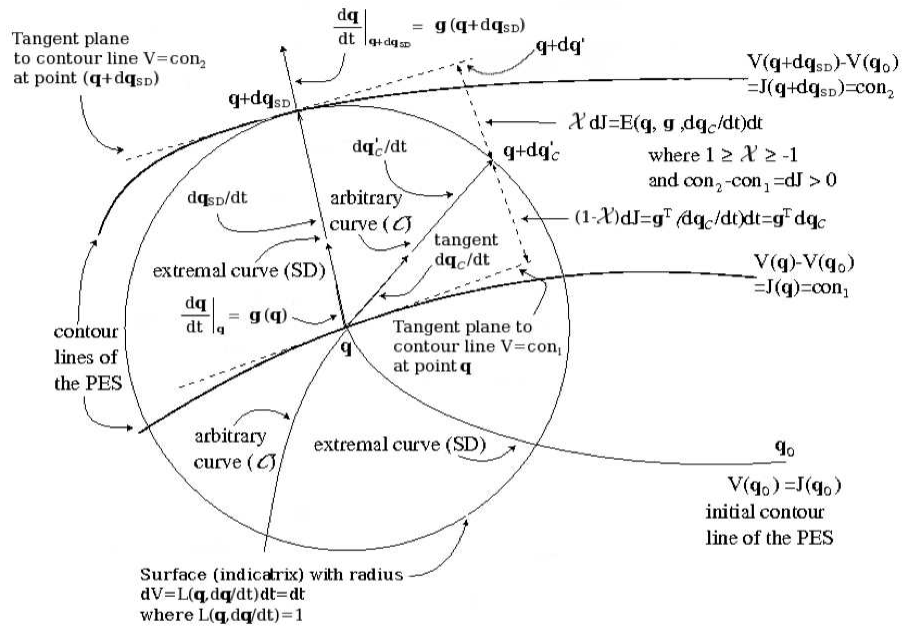
view Only



## REFERENCES

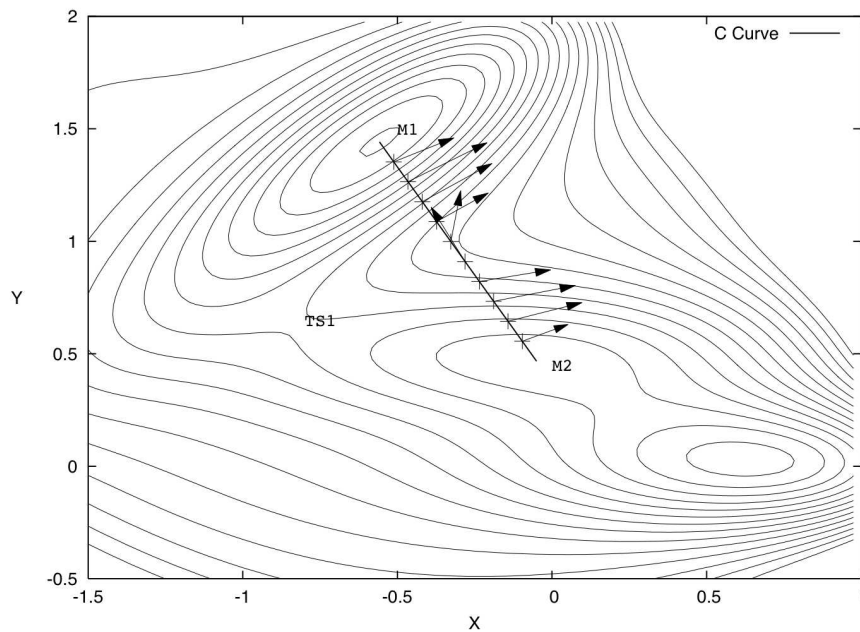
- [1] P. Pulay, *Mol. Phys.* **18**, 473 (1971).
- [2] P. Pulay, *Mol. Phys.* **21**, 329 (1971).
- [3] P. Pulay, *Adv. Chem. Phys.* **69**, 241 (1987).
- [4] P. Pulay, in *Modern Electronic Structure Theory*, edited by D. R. Yarkony (World Scientific, Singapore, 1995), p. 1191.
- [5] K. Fukui, *J. Phys. Chem.* **74**, 4161 (1970).
- [6] W. Quapp, *J. Theor. Comput. Chem.* **2**, 385 (2003).
- [7] D. Heidrich, editor, *The Reaction Path in Chemistry: Current Approaches and Perspectives* (Kluwer, Dordrecht, 1995).
- [8] W. Miller, N. C. Handy, and J. E. Adams, *J. Chem. Phys.* **72**, 99 (1980).
- [9] J. González, X. Giménez, and J. M. Bofill, *J. Phys. Chem. A* **105**, 5022 (2001).
- [10] J. González, X. Giménez, and J. M. Bofill, *Theor. Chem. Acc.* **112**, 75 (2004).
- [11] J. González, X. Giménez, and J. M. Bofill, *Phys. Chem. Chem. Phys.* **4**, 2921 (2002).
- [12] W. Quapp, *J. Mol. Struct. (THEOCHEM)* **695 – 696**, 95 (2004).
- [13] K. Fukui, *Int. J. Quantum Chem., Quantum Chem. Symp.* **15**, 633, (1981).
- [14] R. Crehuet and J. M. Bofill, *J. Chem. Phys.* **122**, 234105 (2005).
- [15] R. Courant and D. Hilbert, *Methods of Mathematical Physics* (Wiley, New York, 1953), Vol. II.
- [16] A. Aguilar-Mogas, X. Giménez, and J. M. Bofill, *Chem. Phys. Lett.* **432**, 375 (2006).
- [17] A. Ulitsky and R. Elber, *J. Chem. Phys.* **92**, 1510 (1990).
- [18] G. Henkelman and H. Jonsson, *J. Chem. Phys.* **113**, 9978 (2000).
- [19] W. E, W. Ren, and E. Vanden-Eijnden, *Phys. Rev. B* **66**, 052301 (2002).
- [20] W. Ren, *Commun. Math. Sci.* **1**, 377 (2003).
- [21] B. Peters, A. Heyden, A. T. Bell, and A. Chakraborty, *J. Chem. Phys.* **120**, 7877 (2004).
- [22] N. González-García, J. Pu, A. González-Lafont, J. M. Lluch, and D. G. Truhlar, *J. Chem. Theory Comput.* **2**, 895 (2006).

- 1  
2  
3  
4  
5  
6  
7  
8  
9  
10  
11  
12  
13  
14  
15  
16  
17  
18  
19  
20  
21  
22  
23  
24  
25  
26  
27  
28  
29  
30  
31  
32  
33  
34  
35  
36  
37  
38  
39  
40  
41  
42  
43  
44  
45  
46  
47  
48  
49  
50  
51  
52  
53  
54  
55  
56  
57  
58  
59  
60
- 
- [23] H. B. Schlegel, in *Encyclopedia of Computational Chemistry*, edited by P. v. R. Schleyer, N. L. Allinger, P. A. Kollman, T. Clark, H. F. Schaefer, III, J. Gasteiger, and P. R. Schreiner (Wiley, Chichester, 1998), Vol. 4, p. 2432.
- [24] M. A. Collins, *Adv. Chem. Phys.* **93**, 389 (1996).
- [25] M. L. McKee and M. Page, in *Reviews in Computational Chemistry*, edited by K. B. Lipkowitz and D. B. Boyd (VCH, New York, 1993), Vol. 4, p. 35.
- [26] K. Ishida, K. Morokuma, and A. Komornicki, *J. Chem. Phys.* **66**, 2153 (1977).
- [27] M. Page and J. W. McIver, *J. Chem. Phys.* **88**, 922 (1988).
- [28] M. Page, C. Doubleday, and J. W. McIver, *J. Chem. Phys.* **93**, 5634 (1990).
- [29] B. C. Garrett, M. J. Redmon, R. Steckler, D. G. Truhlar, K. K. Baldrige, D. Bartol, M. W. Schmidt, and M. S. Gordon, *J. Phys. Chem.* **92**, 1476 (1988).
- [30] K. K. Baldrige, M. S. Gordon, R. Steckler, and D. G. Truhlar, *J. Phys. Chem.* **93**, 5107 (1989).
- [31] V. S. Melissas, D. G. Truhlar, and B. C. Garrett, *J. Chem. Phys.* **96**, 5758 (1992).
- [32] C. Gonzalez and H. B. Schlegel, *J. Chem. Phys.* **90**, 2154 (1989).
- [33] C. Gonzalez and H. B. Schlegel, *J. Phys. Chem.* **94**, 5523 (1990).
- [34] C. Gonzalez and H. B. Schlegel, *J. Chem. Phys.* **95**, 5853 (1991).
- [35] J.-Q. Sun and K. Ruedenberg, *J. Chem. Phys.* **99**, 5257 (1993).
- [36] J.-Q. Sun and K. Ruedenberg, *J. Chem. Phys.* **99**, 5269 (1993).
- [37] J.-Q. Sun, K. Ruedenberg, and G. J. Atchity, *J. Chem. Phys.* **99**, 5276 (1993).
- [38] K. Ruedenberg and J.-Q. Sun, *J. Chem. Phys.* **100**, 6101 (1994).
- [39] F. Eckert and H.-J. Werner, *Theor. Chem. Acc.* **100**, 21 (1998).
- [40] G. A. Bliss, *Lectures on the Calculus of Variations* (The University of Chicago Press, Chicago, 1946).
- [41] H. Rund, *The Hamilton-Jacobi Theory in the Calculus of Variations* (Van Nostrand, London, 1966).
- [42] P. Y. Ayala and H. B. Schlegel, *J. Chem. Phys.* **107**, 375 (1997).
- [43] R. Fletcher, *Practical Methods of Optimization* (Wiley, Chichester, 1987).
- [44] K. Muller and L. D. Brown, *Theor. Chim. Acta* **53**, 75 (1979).
- [45] L. M. Graves, *Am. J. Math.* **52**, 1 (1930).
- [46] M. Hirchs, W. Quapp, and D. Heidrich, *Theor. Chem. Acc.* **112**, 40 (2004).
- [47] M. Hirchs and W. Quapp, *J. Math. Chem.* **36**, 307 (2004).



169x192mm (150 x 150 DPI)

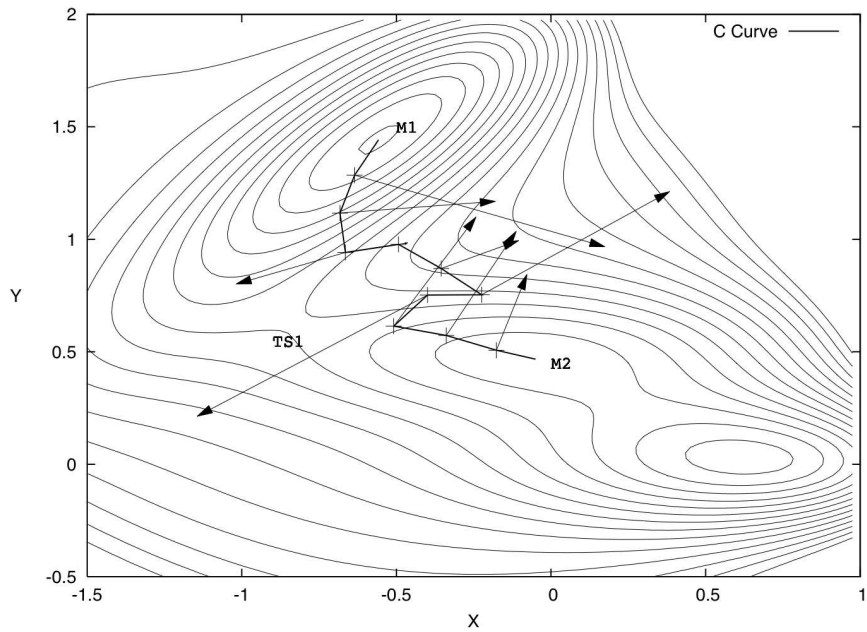




268x207mm (150 x 150 DPI)

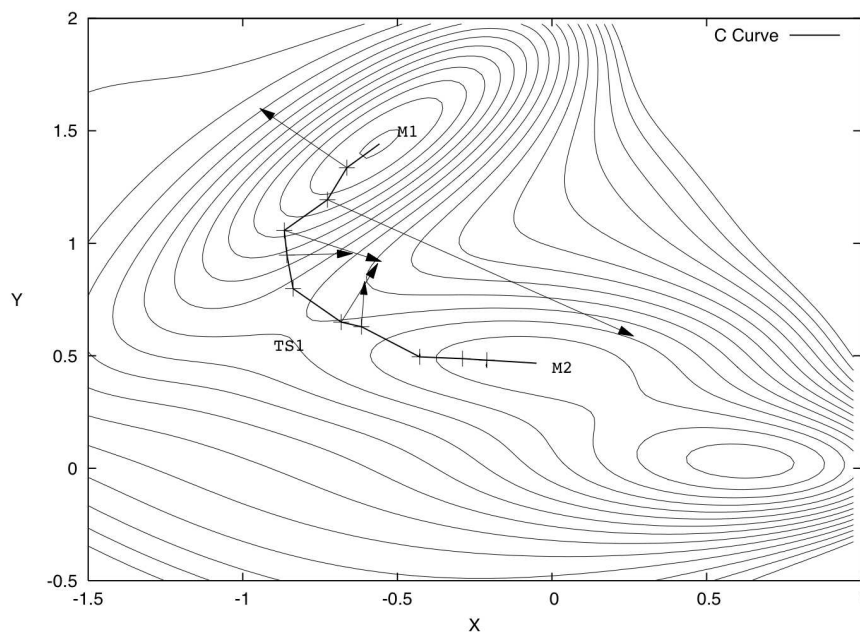
NEW Only

1  
2  
3  
4  
5  
6  
7  
8  
9  
10  
11  
12  
13  
14  
15  
16  
17  
18  
19  
20  
21  
22  
23  
24  
25  
26  
27  
28  
29  
30  
31  
32  
33  
34  
35  
36  
37  
38  
39  
40  
41  
42  
43  
44  
45  
46  
47  
48  
49  
50  
51  
52  
53  
54  
55  
56  
57  
58  
59  
60



268x207mm (150 x 150 DPI)

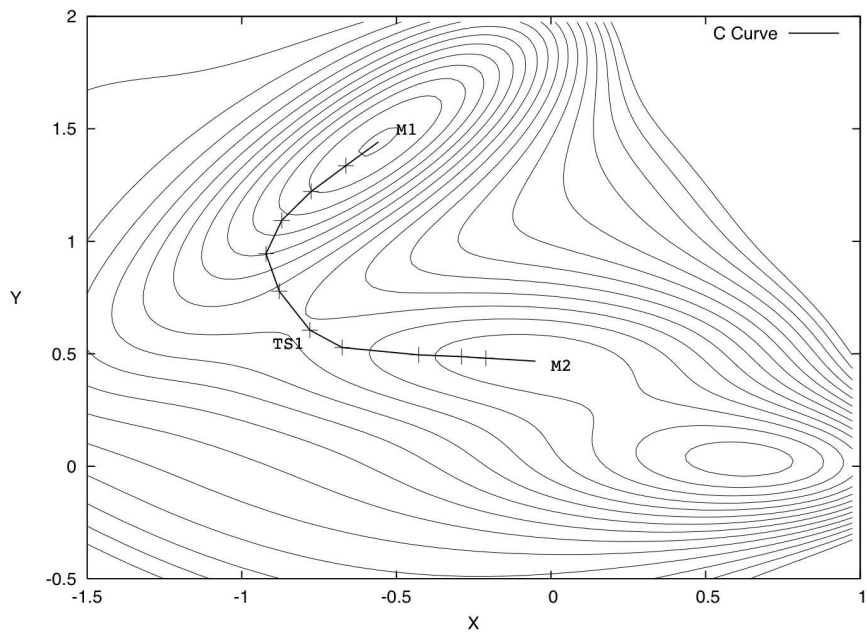
View Only



268x207mm (150 x 150 DPI)

NEW Only

1  
2  
3  
4  
5  
6  
7  
8  
9  
10  
11  
12  
13  
14  
15  
16  
17  
18  
19  
20  
21  
22  
23  
24  
25  
26  
27  
28  
29  
30  
31  
32  
33  
34  
35  
36  
37  
38  
39  
40  
41  
42  
43  
44  
45  
46  
47  
48  
49  
50  
51  
52  
53  
54  
55  
56  
57  
58  
59  
60

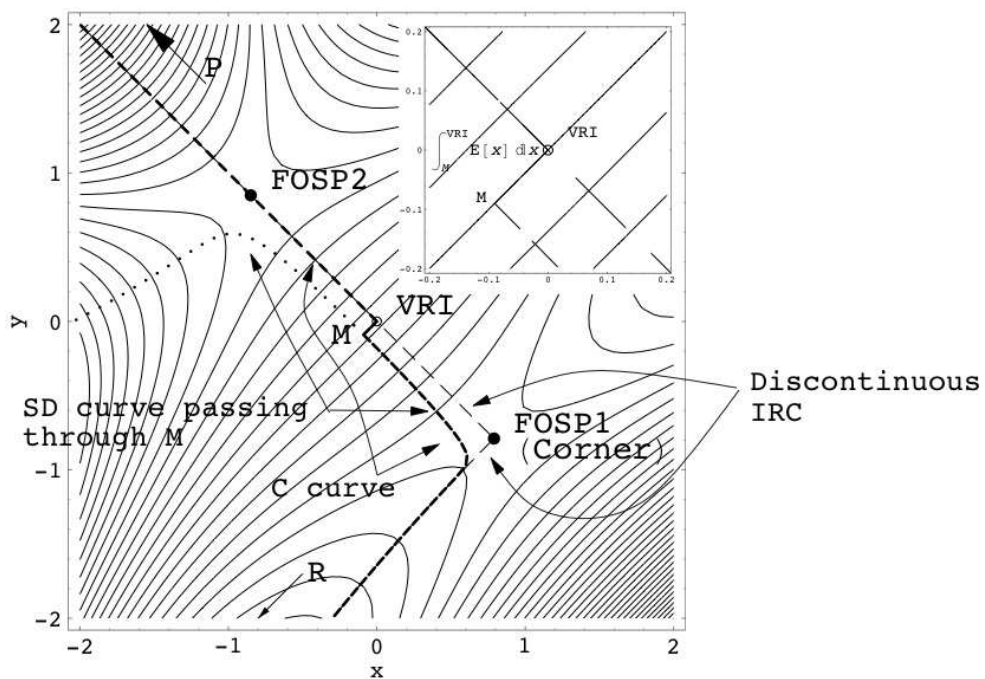


268x207mm (150 x 150 DPI)

View Only



1  
2  
3  
4  
5  
6  
7  
8  
9  
10  
11  
12  
13  
14  
15  
16  
17  
18  
19  
20  
21  
22  
23  
24  
25  
26  
27  
28  
29  
30  
31  
32  
33  
34  
35  
36  
37  
38  
39  
40  
41  
42  
43  
44  
45  
46  
47  
48  
49  
50  
51  
52  
53  
54  
55  
56  
57  
58  
59  
60



143x97mm (150 x 150 DPI)

view Only